Evaluating the use of amber in palaeoatmospheric reconstructions: The carbon-isotope variability of modern and Cretaceous conifer resins

Jacopo Dal Corso [a,b,*], Alexander R. Schmidt [c], Leyla J. Seyfullah [c], Nereo Preto [a], Eugenio Ragazzi [d], Hugh C. Jenkyns [e], Xavier Delclòs [f], Didier Néraudeau [g], Guido Roghi [h]

[a] *Dipartimento di Geoscienze, Università degli Studi di Padova, Via Gradenigo 6, 35131 Padova, Italy*
[b] *Dipartimento di Fisica e Scienze della Terra, Università degli Studi di Ferrara, via Saragat 1, 44122 Ferrara, Italy*
[c] *Abteilung Geobiologie, Georg-August-Universität Göttingen, Goldschmidtstraße 3, 37077 Göttingen, Germany*
[d] *Dipartimento di Scienze del Farmaco, Università degli Studi di Padova, L.go Meneghetti 2, 35131 Padova, Italy*
[e] *Department of Earth Sciences, University of Oxford, South Parks Road, Oxford OX1 3AN, UK*
[f] *Departament of ''Ciències de la Terra i de l'Oceà'', Facultat de Ciències de la Terra, Universitat de Barcelona, Marti i Franques s/n, 08028 Barcelona, Spain*
[g] *Université Rennes 1, Géosciences, CNRS UMR 6118, Campus de Beaulieu, Bat. 15, 263 Avenue du General Leclerc, Rennes Cedex, France*
[h] *Istituto di Geoscienze e Georisorse (IGG-CNR), via Gradenigo 6, 35131 Padova, Italy*

Abstract

Stable carbon-isotope geochemistry of fossilized tree resin (amber) potentially could be a very useful tool to infer the composition of past atmospheres. To test the reliability of amber as a proxy for the atmosphere, we studied the variability of modern resin $\delta^{13}C$ at both local and global scales. An amber $\delta^{13}C$ curve was then built for the Cretaceous, a period of abundant resin production, and interpreted in light of data from modern resins. Our data show that hardening changes the pristine $\delta^{13}C$ value by causing a ^{13}C-depletion in solid resin when compared to fresh liquid–viscous resin, probably due to the loss of ^{13}C-enriched volatiles. Modern resin $\delta^{13}C$ values vary as a function of physiological and environmental parameters in ways that are similar to those described for leaves and wood. Resin $\delta^{13}C$ varies between plant species and localities, within the same tree and between different plant tissues by up to 6‰, and in general increases with increasing altitudes of the plant-growing site. We show that, as is the case with modern resin, Cretaceous amber $\delta^{13}C$ has a high variability, generally higher than that of other fossil material. Despite the high natural variability, amber shows a negative 2.5–3‰ $\delta^{13}C$ trend from the middle Early Cretaceous to the Maastrichtian that parallels published terrestrial $\delta^{13}C$ records. This trend mirrors changes in the atmospheric $\delta^{13}C$ calculated from the $\delta^{13}C$ and $\delta^{18}O$ of benthic foraminiferal tests, although the magnitude of the shift is larger in plant material than in the atmosphere. Increasing mean annual precipitation and pO_2 could have enhanced plant carbon-isotope fractionation during the Late Cretaceous, whereas changing pCO_2 levels seem to have had no effect on plant carbon-isotope fractionation. The results of this study suggest that amber is a powerful fossil plant material for palaeoenvironmental and palaeoclimatic reconstructions. Improvement of the resolution of the existing data coupled with more detailed information about botanical source

* Corresponding author at: Hanse-Wissenschaftskolleg (HWK), Lehmkuhlenbusch 4, 27753 Delmenhorst, Germany, and Leibniz Center for Tropical Marine Ecology (ZMT), Fahrenheitstraße 6, 28359 Bremen, Germany.
   E-mail address: jacopo.dalcorso@gmail.com (J. Dal Corso).

and environmental growing conditions of the fossil plant material will probably allow a more faithful interpretation of amber $\delta^{13}C$ records and a wider understanding of the composition of the past atmosphere.

1. INTRODUCTION

Since C3 plants take up atmospheric CO_2 during photosynthesis and record its carbon-isotope signature, fossil plant remains (such as leaves and wood) can be used to reconstruct the palaeoatmosphere (e.g. Arens et al., 2000; Gröcke, 2002; Bechtel et al., 2008; Diefendorf et al., 2010). Plants discriminate against ^{13}C during photosynthesis, and the degree of ^{13}C fractionation ($\Delta^{13}C_P$) depends not only on plant physiology but also on a number of environmental factors and post-photosynthetic $\Delta^{13}C_P$ processes, which determine the $\delta^{13}C$ of plant tissues (Arens et al., 2000; Diefendorf et al., 2010; Schubert and Jahren, 2012). The pristine carbon-isotope composition of wood and leaves, the most commonly used tissues in chemostratigraphic analysis, is further changed by diagenesis, through which moieties with different $\delta^{13}C$ signatures are selectively removed (e.g. van Bergen and Poole, 2002; Bechtel et al., 2002). Natural variability and diagenesis make the reconstructions of past atmospheric carbon-isotope composition based on plant $\delta^{13}C$ analysis difficult because, particularly in deep-time studies, it is often impossible to separate physiological and environmental effects from atmospheric signals and evaluate the diagenetic effect (Diefendorf et al., 2010). The $\delta^{13}C$ of fossil wood and leaves ($\delta^{13}C_{WOOD}$ and $\delta^{13}C_{LEAF}$) has been successfully used to infer changes in the carbon-isotope composition of past atmosphere–ocean systems, an approach supported by the evidence of $\delta^{13}C$ excursions synchronously recorded in both terrestrial organic matter and marine carbonates (e.g. Gröcke, 2002; Strauss and Peters-Kottig, 2003; Dal Corso et al., 2011). Records of $\delta^{13}C_{WOOD}$ and $\delta^{13}C_{LEAF}$ parallel those of marine carbonates and can record global long- and short-term perturbations of the carbon cycle, such as the Middle–early Late Triassic 3‰ positive $\delta^{13}C$ long-term trend (Dal Corso et al., 2011), and the Jurassic and Cretaceous positive and negative shifts associated with oceanic anoxic events (OAEs; e.g. Gröcke, 2002; Hesselbo et al., 2007).

As a biochemical product of terrestrial plants, amber (fossil tree resin) is expected to record the same $\delta^{13}C$ shifts recorded by other plant compounds and tissues. Amber is an extraordinary medium for the preservation of animals, plants and fungi that are otherwise rare in the fossil record. It is resistant to diagenesis and can maintain its original chemical and isotopic composition and for this reason is thought to be a very powerful tool for reconstruction of the palaeoatmosphere and the palaeoenvironment (Murray et al., 1998; McKellar et al., 2011; Dal Corso et al., 2011, 2013; Aquilina et al., 2013; Tappert et al., 2013). It has been shown that amber $\delta^{13}C$ ($\delta^{13}C_{AMBER}$) falls in the range of typical modern C3 plants and may reveal information about climate and environment at the time of

resin exudation, for example changes in plant carbon-isotope discrimination linked to environmental stresses such as insect infestation or water availability (Murray et al., 1994, 1998; Nissenbaum and Yakir, 1995; McKellar et al., 2008, 2011; Dal Corso et al., 2011, 2013; Tappert et al., 2013). However, contrary to that of wood and leaf, less research has focused on developing amber as a palaeoatmosphere proxy (Tappert et al., 2013). In addition, the lack of sufficient data on the carbon-isotope geochemistry of modern resin, i.e. on the variation of $\delta^{13}C_{RESIN}$ (resin $\delta^{13}C$) under different environmental conditions, renders interpretation of $\delta^{13}C_{AMBER}$ problematic.

Here, as a test case, we explore the value of $\delta^{13}C_{AMBER}$ as a proxy for the Cretaceous atmosphere. We studied the variability of modern $\delta^{13}C_{RESIN}$ using samples produced by extant conifers from different temperate to tropical environments in order to understand whether resin carbon-isotope behaviour is similar to that of plant tissues. We do not aim to explain the biological and biochemical reasons behind the observed behaviour of modern $\delta^{13}C_{RESIN}$ but rather to highlight the patterns and variability that could hamper palaeoclimatic reconstructions and chemostratigraphy. New Cretaceous $\delta^{13}C_{AMBER}$ data, coupled with a compilation of published data, were compared in order to combine terrestrial and marine $\delta^{13}C$ records, and interpreted in light of both present-day isotopic variability and the Cretaceous climate.

2. MATERIAL AND METHODS

2.1. Methodical background: Factors controlling the $\delta^{13}C$ of modern C3 plants

The $\delta^{13}C$ of C3 plants ($\delta^{13}C_P$) was calculated according to the model of Farquhar et al. (1989) [Eq. (1)] and depends on the $\delta^{13}C_{ATM}$ ($\delta^{13}C$ of the atmosphere) and on the ratio between the pCO_2 inside the leaves and the atmospheric pCO_2 (c_i/c_a):

$$\delta^{13}C_P = \delta^{13}C_{ATM} - a - (b-a)^*c_i/c_a \tag{1}$$

where a is the fractionation during diffusion of the CO_2 from the atmosphere into leaves and is fixed at 4.4‰; b is the fractionation during ribulose-1,5-bisphosphate carboxylase/oxygenase (RuBisCO) carboxylation and has values of 26–30‰ (e.g. Farquhar et al., 1989; Arens et al., 2000; Schubert and Jahren, 2012); and c_i/c_a is the ratio between intercellular and atmospheric pCO_2. The c_i/c_a usually varies between 0.65 and 0.8 with a maximum range between 0.3 and 0.9 (e.g. Farquhar et al., 1989; Arens et al., 2000).

Post-photosynthetic fractionation also occurs during the biosynthesis of plant compounds, which consequently have

different $\delta^{13}C$ signatures (Badeck et al., 2005). In general, non-photosynthetic tissues are more ^{13}C-enriched by 1–3‰ than photosynthetic tissues such as leaves (Cernusak et al., 2009).

Studies suggested that the $\delta^{13}C_P$ is primarily controlled by $\delta^{13}C_{ATM}$ (Arens et al., 2000; Jahren et al., 2008). However, additional strong dependence of $\Delta^{13}C_P$ upon other factors complicates the $\delta^{13}C_P - \delta^{13}C_{ATM}$ relationship (e.g. Nordt et al., 2016). The c_i/c_a ratio in [Eq. (1)] is regulated by stomatal conductance, which is governed by the closing or opening of the stomata. Stomatal conductance can be influenced by many environmental factors, particularly water availability and pCO_2. For example, Diefendorf et al. (2010) and Kohn (2010) showed that $\Delta^{13}C_P$ is strongly correlated to mean annual precipitation (MAP) and plant functional types. Both these studies found an increase of $\Delta^{13}C_P$ with increase of MAP. This dependence was modelled and tested in the fossil record (Diefendorf et al., 2015; Kohn, 2016). Schubert and Jahren (2012) gave evidence that $\Delta^{13}C_P$ by C3 plants grown in environmentally controlled chambers hyperbolically increases with increasing ambient pCO_2 levels. The model of Schubert and Jahren (2012) was tested against ice-core records and used to reconstruct pCO_2 during the Palaeocene–Eocene Thermal Maximum (PETM) (Schubert and Jahren, 2013, 2015). In contrast to this model, recent studies found no or negligible pCO_2 dependence over long time scales (Kohn, 2016), keeping open the question as to whether MAP or pCO_2 predominantly control $\Delta^{13}C_P$. Moreover, Berner et al. (2000) and Beerling et al. (2002) experimentally demonstrated an increase of $\Delta^{13}C_P$ with increase in pO_2 levels. Subsequently, Tappert et al. (2013) proposed the use of fossil plant $\delta^{13}C$ to reconstruct palaeo-pO_2, assuming that, in ambient air, $\Delta^{13}C_P$ is proportional to pO_2 and that physiological adaptations did not occur through time. Although there is no agreement as to which factor is most important in determining the carbon-isotope composition of modern plants, all these factors must be taken into account to correctly interpret the carbon-isotope shifts registered by fossil plant material in the geological record (Diefendorf et al., 2010; Schubert and Jahren, 2012; Kohn, 2016).

2.2. Modern and Cretaceous resin samples

Modern resin samples from the USA and New Caledonia were collected by A. R. Schmidt and L. J. Seyfullah in 2005, 2010 and 2011 (USA) and in 2005 and 2011 (New Caledonia). J. Dal Corso, G. Roghi and E. Ragazzi collected resins from different conifers growing at the Botanical Gardens of the University of Padova in 2010. In Padova, *Araucaria heterophylla* resin, leaves and wood were also collected at different heights from the base of the tree. Both liquid-viscous and solid resins were sampled. Carbon-isotope data, plant species, altitude and geographic provenance are summarized in Fig. 1 and Supplementary Table 1.

The Cretaceous amber analysed for this study derives from different deposits in Spain (25 samples), France (10 samples), and from the Grassy Lake deposit (5 samples)
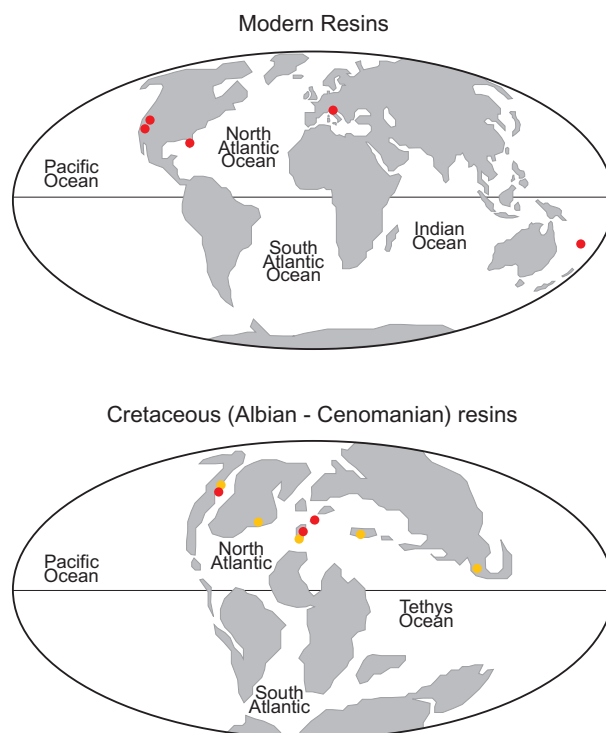

Fig. 1. Location of the sampling sites of modern resins (A) and Cretaceous amber (B) analysed for carbon isotopes. Red dots = this study; orange dots = previous studies (Nissenbaum and Yakir, 1995; Dal Corso et al., 2013; Tappert et al., 2013). (For interpretation of the references to colour in this figure legend, the reader is referred to the web version of this article.)

in Canada (Fig. 1). Their origin and ages are summarized in Supplementary Table 2 and Supplementary Fig. 1. Spanish amber samples were collected by X. Delclòs and are stored at the University of Barcelona, Spain. They derive from several Aptian–Maastrichtian deposits from the Central Asturian Depression, the West and East areas of the Basque-Cantabrian Basin, the Maestrazgo (=Maestrat) Basin and the Castilian Platform. The age of these deposits is mainly constrained by pollen and spores and includes uncertainties from ~1 up to ~18 Myrs (see Supplementary Table 2 and Supplementary Fig. 1; Peñalver and Delclòs, 2010; Barrón et al., 2015). Samples of French amber come from the collection of D. Néraudeau stored at the Université de Rennes, France. The Late Albian-Early Cenomanian and Santonian ages of amber samples from different localities in France are well constrained by pollen, spores, dinoflagellates, foraminifers, ostracods and rudists (Peyrot et al., 2005; Batten et al., 2010), with uncertainties of ~1 up to ~3 Myrs (see Supplementary Table 2). Grassy Lake amber was collected and provided by A. Wolfe (University of Alberta) and is Campanian in age, according to McKellar et al. (2008) and Tappert et al. (2013). $\delta^{13}C_{AMBER}$ data of Cretaceous amber were coupled with previously published $\delta^{13}C_{RESIN}$ data from Nissenbaum and Yakir (1995), Dal Corso et al. (2013) and Tappert et al. (2013). The ages of some of these deposits, namely the Levantine amber from Israel and Lebanon and the San Just

amber from Spain, have been revised according to recent stratigraphic data. The Lebanese amber-bearing deposits with bioinclusions (entrapped fossilized organisms) are from the Lower Cretaceous: Ante-Jezzinian (Maksoud et al., 2014), i.e., ante Lower Bedoulian (Bedoulian being Upper Barremian–Lower Aptian). Deposits of Cretaceous Lebanese amber with bioinclusions are situated in the Chouf Sandstone Formation (= Grès de Base or C1 in older usages), under the recently defined Jezzinian Regional-Stage (uppermost Barremian–lower Aptian). The lower boundary of the Jezzinian is probably within the uppermost Barremian (Maksoud et al., 2014). According to new biostratigraphical data, the oldest Lebanese amber deposits with bioinclusions are Early Barremian and the youngest are intra-Barremian (Maksoud et al., 2016). The San Just amber outcrop is located in the Maestrazgo Basin and is included in the Escucha Fm. of the Utrillas Group (SSS – Superior Sedimentary Succession; Rodríguez-López et al., 2009). It was dated as Middle-Upper Albian by Villanueva-Amadoz et al. (2010), based on the palynological fossil record and it is now constrained to the Upper Albian by comparison with similar deposits in the Basque–Cantabrian Basin with similar fossil content (Barrón et al., 2015).

2.3. $\delta^{13}C_{RESIN}$ analysis

Clean sub-millimetric fragments of the collected modern resins were separated under the microscope to perform $\delta^{13}C$ analysis. Close attention was paid in order to select clear resin portions to avoid the presence of microscopic inclusions. The $\delta^{13}C$ analysis was performed on a Thermo Scientific Delta V Advantage Isotope Ratio Mass Spectrometer in continuous flow mode, coupled with a Flash 2000 Elemental Analyser and a ConFlo IV interface. 0.03–0.05 mg of resin were weighed in a tin capsule and fed to the Elemental Analyser. The Mass Spectrometer analysed CO_2 gas resulted from high temperature combustion. On the basis of a long-term mean of >30 tin-cap analyses, a blank correction was applied to the raw data and the results were calibrated against repeated analyses of IAEA-CH6 and IAEA-CH7 international standards, whose $\delta^{13}C$ is respectively −10.449‰ and −32.151‰ (Coplen et al., 2006). The long-term internal reproducibility was estimated on repeated analyses of an internal standard (C3 plant sucrose) and is better than 0.15‰ (1σ).

Samples of Cretaceous amber were first crushed with an agate mortar to obtain a fine powder. Repeated analyses on different portions of single Cretaceous amber specimens have shown that the $\delta^{13}C$ is remarkably homogeneous within the same piece (Dal Corso et al., 2013). We thus consider the measured $\delta^{13}C$ as representative of the entire amber sample. The amber powder was placed in a polypropylene tube and treated with 3 M HCl to remove possible residual carbonates from the sediments where the amber had been embedded. Samples were then rinsed with deionized water until neutrality was reached and were oven-dried at 50 °C. 1.5–2 mg of amber powder were weighed in tin capsules and fed into the Elemental Analyzer. $\delta^{13}C$ analysis was performed using a Carlo Erba NA 1108 Elemental

Analyzer coupled to a SERCON Geo 20/20 IRMS running in continuous flow mode with a He carrier gas (flow rate 100 ml per min). The reproducibility of the analyses was estimated using an internal standard (alanine) routinely checked against international standards IAEA-CH-6 and IAEA-CH-7 and traceable back to the VPDB standard. All results are accurate to better than ±0.15‰ (1σ).

2.4. Meta-analysis of terrestrial and marine carbon-isotope data

The amber data generated in this study have been coupled with the published $\delta^{13}C_{AMBER}$ data from Tappert et al. (2013), Nissenbaum and Yakir (1995) and Dal Corso et al. (2013), allowing improved resolution of the $\delta^{13}C_{AMBER}$ record. To compare the variability of $\delta^{13}C_{AMBER}$ with other Cretaceous C3 plant material we used the recently compiled ISOORG database (Nordt et al., 2016). ISOORG comprises $\delta^{13}C$ data ($\delta^{13}C_{ISOORG}$) of plant material including wood, leaf, charcoal, coal, and bulk terrestrial organic matter from various geographical locations. We also built a low-resolution wood $\delta^{13}C$ ($\delta^{13}C_{WOOD}$) record coupling the Lower Cretaceous wood data extracted from ISOORG (Nordt et al., 2016) with the Maastrichtian data of Salazar-Jaramillo et al. (2016). Before processing data we excluded from ISOORG all $\delta^{13}C_{AMBER}$ data; all of

Table 1
Plant species from which resin was collected, resin mean carbon-isotope values for each species (mean ± standard deviation (SD)) and sample size.

Species	$\delta^{13}C \pm SD$ (‰)	n.
Abies concolor	−23.7	1
Abies magnifica	−23.6 ± 1.1	2
Agathis lanceolata	−24.5 ± 0.2	2
Agathis moorei	−25.9 ± 0.4	2
Agathis ovata	−25.7	1
Araucaria (all species listed below)	−27.1 ± 1.4	13
Araucaria columnaris	−26.3 ± 1.3	4
Araucaria excelsa	−28.8 ± 0.8	4
Araucaria humboldtensis	−26.3 ± 0.7	4
Araucaria rulei	−27.6	1
Cedrus deodara	−24.9 ± 0.5	2
Cupressus arizonica	−29.8 ± 0.1	2
Falcatifolium taxoides	−24.4	1
Juniperus occidentalis	−27.4	1
Picea abies	−27.7	1
Pinus (all species listed below)	−26.9 ± 1.7	55
Pinus balfouriana	−24.3 ± 0.6	2
Pinus coulteri	−25.8 ± 0.32	3
Pinus edulis	−24 ± 0.7	3
Pinus elliottii	−28.3 ± 0.2	3
Pinus jeffreyi	−28.2 ± 1.1	10
Pinus lambertiana	−26.5 ± 1	5
Pinus longaeva	−24.6	1
Pinus monophylla	−24.9 ± 0.9	5
Pinus monticola	−28 ± 2	2
Pinus muricata	−28.2 ± 0.9	8
Pinus ponderosa	−27.2 ± 1.3	9
Pinus radiata	−26.5 ± 0.8	2
Pinus sabiniana	−27.2 ± 0.7	2

Table 2
Standard deviation (SD), interquartile range (IQR) and sample size (n.) of δ¹³C data of modern resin and leaf, and Cretaceous amber, wood and other mixed C3 plant material (from ISOORG; TOM = bulk terrestrial organic matter). For the Cretaceous, SD and IQR have been also calculated per each 5 Myrs age bin from 65 Ma to 145 Ma (see text and Nordt et al., 2016 for explanations). Bins not listed in the table contain no data. ISOORG and wood data are taken from Nordt et al. (2016) and Salazar-Jaramillo et al. (2016).

| Age	Type	Mean (‰)	SD (‰)	IQR (‰)	n.
Modern	Resin	−26.7	1.77	2.7	85
	Leaf	−28.4	2.52	3.6	513
Cretaceous	Amber	−22.3	1.95	2.5	201
	C3 Plant	−24.2	1.31	1.4	1384
	Charcoal	−22.9	1.55	2	192
	Coal	−24.2	1.43	1.23	95
	Leaf and cuticle	−24.7	1.72	2.14	16
	TOM	−24.4	0.98	1.1	874
	Wood	−23.1	1.31	1.47	207
AGE bin	Type		SD (‰)	IQR (‰)	*n.*
65 Ma	C3 Plant (TOM, leaf, coal)	−24.5	0.88	1.08	677
70 Ma	Amber	−23.7	1.79	2.60	40
	C3 Plant (TOM, leaf, coal)	−25.9	1.17	1.60	43
	Wood	−25.2	1,32	1,80	27
75 Ma	Amber	−23.5	1.39	1.75	51
	C3 Plant (TOM)	−24.7	0.30	0.38	5
85 Ma	C3 Plant (TOM)	−24	0.31	0.42	14
90 Ma	Amber	−22.1	1.10	1.60	36
	C3 Plant (TOM)	−24.1	0.51	0.50	9
95 Ma	C3 Plant (TOM)	−23.6	0.73	1.12	167
100 Ma	Amber	−21.1	0.98	1.33	11
105 Ma	Amber	−22	1.33	1.85	14
110 Ma	C3 Plant (leaf)	−24.8	2.03	1.88	8
125 Ma	Wood	−22.2	1.15	1.78	19
130 Ma	Amber	−20.8	1.20	2.10	25
	Wood	−22.8	0.93	1.29	89
135 Ma	C3 Plant (coal, charcoal)	−22.9	1.49	1.78	231
	Wood	−23.3	1.04	1.36	35
140 Ma	C3 Plant (coal, wood)	−23.6	1.56	2.18	87
	Wood	−22.9	0.87	1,05	37
145 Ma	Wood	−23.6	0.45	0.69	12
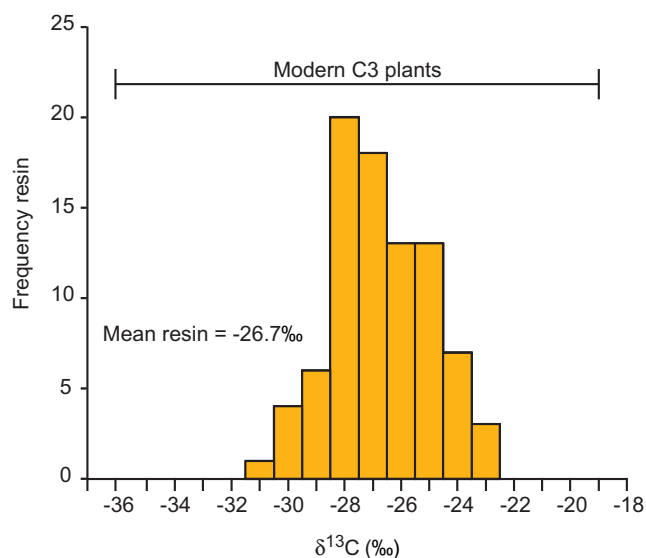
Fig. 2. Distribution of modern resin δ¹³C (orange histogram) and range of variability of modern C3 plants from Cerling and Harris (1999) and Tipple and Pagani (2007). (For interpretation of the references to colour in this figure legend, the reader is referred to the web version of this article.)

which were already included in our compilation. Some of the amber deposits described here have age uncertainties of several millions of years, especially in the case of the mid-Cretaceous Spanish ambers (Supplementary Table 2 and Supplementary Fig. 1). These uncertainties depend on the fact that Cretaceous amber is commonly found in continental (fluvial sediments, coal deposits) or coastal (brackish estuarine/lagoonal) deposits that lack age-significant fossils. For this reason and to allow comparison with the ISOORG database, $\delta^{13}C_{AMBER}$ data were placed into 5 Myrs-age bins following the criteria used by Nordt et al. (2016). Amber with age uncertainty larger than the bin was excluded. The same procedure was used also for $\delta^{13}C_{WOOD}$ from Salazar-Jaramillo et al. (2016). Box-and-whiskers plots for $\delta^{13}C_{AMBER}$, $\delta^{13}C_{WOOD}$ and $\delta^{13}C_{ISOORG}$ data were built for each age bin with a sample size of at least 5 (Krzywinski and Altman, 2014). To compare the terrestrial $\delta^{13}C$ signal to the marine $\delta^{13}C$ signal we took marine carbonate data from the database compiled by Prokoph et al. (2008) and Bodin et al. (2015). We used $\delta^{13}C$ and $\delta^{18}O$ data from benthic and planktonic foraminifera and belemnites. Terrestrial $\delta^{13}C$ data were also compared to the $\delta^{13}C_{ATM}$, which was estimated from the $\delta^{13}C$ and $\delta^{18}O$ of benthic foraminifera using the equations proposed by Tipple et al. (2010). A third-degree polynomial curve was fitted to the data to compare the terrestrial and marine carbonate $\delta^{13}C$ records. Prediction intervals for individual observations hold about 95% of data. Polynomial curve fitting by the least-squares method and prediction intervals were obtained with JMP software, version 10 (SAS Institute Inc., Cary, NC, USA).

3. RESULTS

3.1. Modern resin $\delta^{13}C$

The $\delta^{13}C$ of all the analysed modern resins varies from −31.6‰ to −22.8‰ (mean ± SD = −26.7 ± 1.8‰, $n = 84$; Table 1). $\delta^{13}C_{RESIN}$ values obtained in this study show a normal distribution with a mean of −26.7‰ (Fig. 2). The mean $\delta^{13}C_{RESIN}$ is more ^{13}C-enriched than the mean global leaf $\delta^{13}C$ (−28.5‰ calculated from data of Diefendorf et al., 2010; Fig. 3A). A statistically significant difference (p value = 0.001) exists between liquid–viscous resin and solid resin, the former having more ^{13}C-enriched values (mean −25.9‰) than the latter (mean −27.1‰) (Fig. 3A). Resin has $\delta^{13}C$ values systematically more ^{13}C-enriched by 1–2.3‰ than those of bulk leaf and wood samples collected from the same branch at the same tree height in *Araucaria heterophylla*, *Picea abies* and *Cupressus arizonica* (Fig. 3B). Resin, wood and leaves collected from a single tree of *Araucaria heterophylla* at different heights also possess variable $\delta^{13}C$ signatures (Fig. 3C). Differences of up to 6‰ exist between the mean $\delta^{13}C$ of resins from different plant species (Table 1). The $\delta^{13}C_{RESIN}$ from different tree genera growing at the same altitude in the same locality (Padova, Italy) differs by about 2–5‰ (Fig. 3B). Liquid–viscous and solid resin $\delta^{13}C$ of *Pinus* and *Araucaria* significantly increases with increasing altitude of the sampling site (Fig. 4; liquid–viscous resin, $R = 0.632$, p value

<0.001; Solid resin of *Pinus* and *Araucaria*, $R = 0.634$, p value <0.001). Similar correlation was also observed between $\delta^{13}C_{LEAF}$ and altitude ($R = 0.59$; Körner et al., 1988). The $\delta^{13}C_{RESIN}$ values for the most represented genera show that *Pinus* resin is statistically indistinguishable from *Araucaria* resin (p value = 0.6, Students' t-test; Table 1).

3.2. Cretaceous amber $\delta^{13}C$

The $\delta^{13}C$ of amber from Spain varies between −17‰ and −24.2‰ (mean = −20.1 ± 1.8‰) in the range expected for C3 plant resins (Table 2). Similarly, $\delta^{13}C$ of amber from France and Canada ranges from −18.5‰ to −23.5‰ (mean = −21.1 ± 1.9‰) and from −21.4‰ to −23.4‰ (mean = −22.7 ± 0.8‰), respectively (Table 2). The compiled Cretaceous amber and ISOORG $\delta^{13}C$ values show a normal distribution (Fig. 5A). On average, amber is more ^{13}C-enriched (mean = −22.3‰ ± 1.9‰) than Cretaceous C3 plant material (mean = −24.2‰ ± 1.3‰) and wood (mean = −23.1‰ ± 1.3‰) (Fig. 5B). Cretaceous $\delta^{13}C_{AMBER}$ data are more dispersed than $\delta^{13}C$ values of C3 plant material: the box-and-whisker plots (Fig. 5B) show the interquartile range (IQR) of $\delta^{13}C_{AMBER}$ to be much larger (2.5‰, Table 2) than $\delta^{13}C_{ISOORG}$ (1.4‰). F-test for the equality of variances indicates that the variances of $\delta^{13}C_{AMBER}$ and $\delta^{13}C_{ISOORG}$ are significantly different ($p < 0.0001$). SD and IQR were calculated for each age bin (Table 2) and show that $\delta^{13}C_{AMBER}$ is generally more dispersed then the $\delta^{13}C_{ISOORG}$ and $\delta^{13}C_{WOOD}$. Amber, wood and ISOORG data show that latest Cretaceous (Maastrichtian) $\delta^{13}C$ values are more ^{13}C-depleted than those of the Early Cretaceous (Hauterivian–Barremian) by 2.5–3‰ (Fig. 6). The marine $\delta^{13}C$ record from whole rock, belemnite, and foraminifera (Prokoph et al., 2008; Bodin et al., 2015) shows a pattern that only partially matches the terrestrial records (Fig. 6). The $\delta^{13}C_{ATM}$ calculated from benthic foraminifera shows a decrease of approx. 1‰ from the Aptian to the Maastrichtian that mirrors the decrease (2.5–3‰) shown by terrestrial plants (Fig. 7).

4. DISCUSSION

4.1. Modern resin

4.1.1. Effect of resin hardening on the $\delta^{13}C_{RESIN}$

To obtain reliable information from the carbon-isotope geochemistry of resin on the physiology of plants and the environmental conditions under which they grow, it is necessary to understand whether the measured $\delta^{13}C_{RESIN}$ values actually represent the pristine composition at the time of resin biosynthesis. After exudation, resin is composed of up to 50% of a volatile fraction (mainly monoterpenes and sesquiterpenes). The volatile fraction is lost rapidly on exposure of resin to air and sunlight, whereas the non-volatile fraction (mainly diterpene acids in conifer resin) undergoes polymerization (cross-linking and isomerization) with the formation of high-molecular-weight polymers (Langenheim, 1990; Scalarone et al., 2003; Lambert et al.,
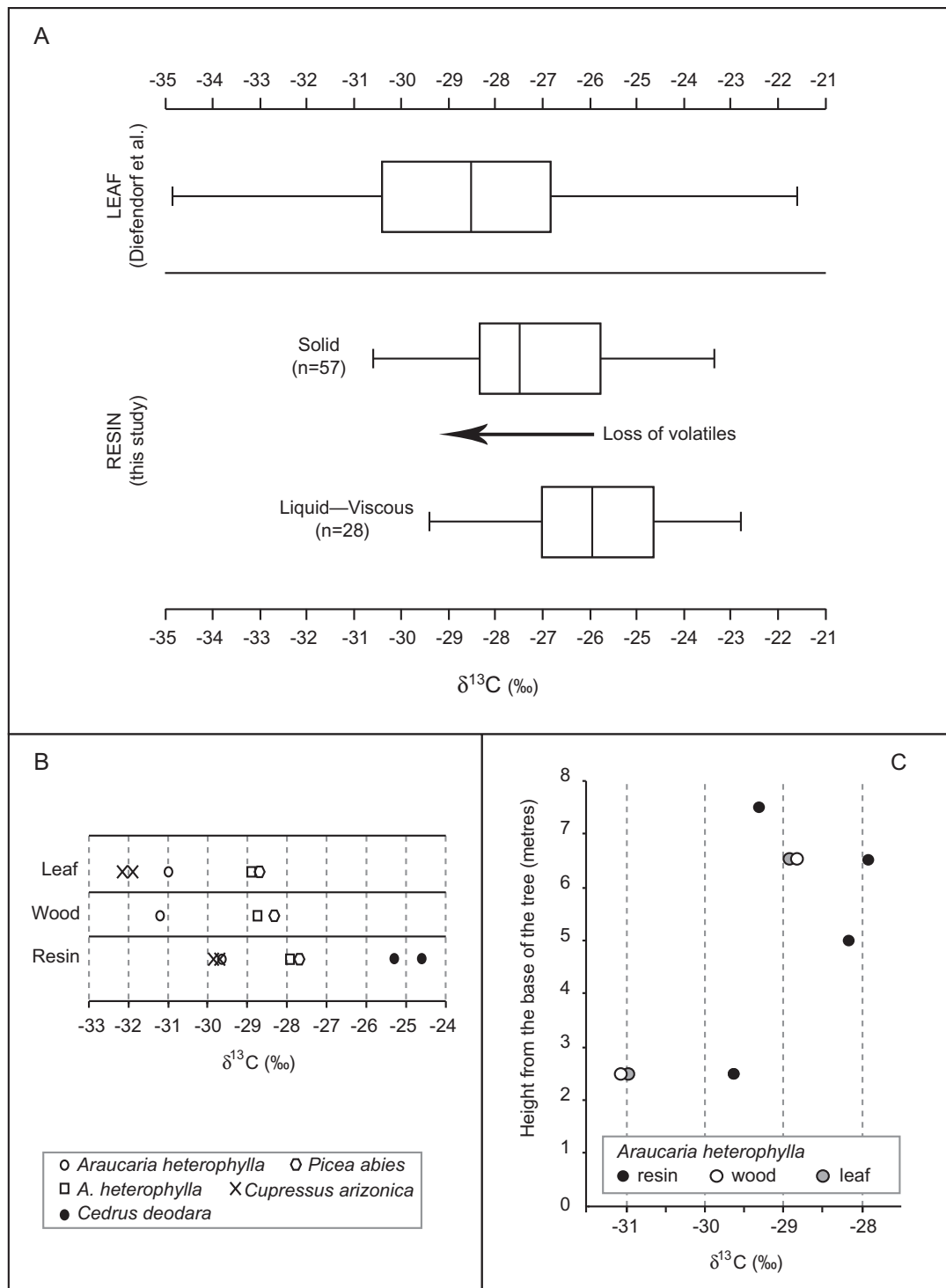
Fig. 3. (A) Carbon-isotope composition of liquid–viscous vs solid modern resin (Students' t-test p value = 0.001). Resin data are compared to a compilation of leaf data taken from Diefendorf et al. (2010). Data are represented as box-and-whiskers plots in order to highlight differences in distribution. The bars represent the first and fourth quartile, the box represents the second and third quartile, and the mid-line is the median. All investigated species are considered. Variation of the carbon-isotope composition (B) of solid resin, wood and leaves from different trees (two trees of *Araucaria heterophylla*, a *Picea abies* tree and a *Cupressus arizonica* tree) and (C) of solid resin collected from a single tree of *Araucaria heterophylla* at different heights. Samples in boxes (B) and (C) were collected in the Botanical Garden of the University of Padova.

2008; Ragazzi and Schmidt, 2011). This selective removal of moieties points to a possible change of the bulk $\delta^{13}C_{RESIN}$ during resin hardening (Dal Corso et al., 2011). Our dataset

comprises both liquid–viscous resins sampled shortly after exudation and solid resins that already had hardened at the site of exudation. A statistically significant difference
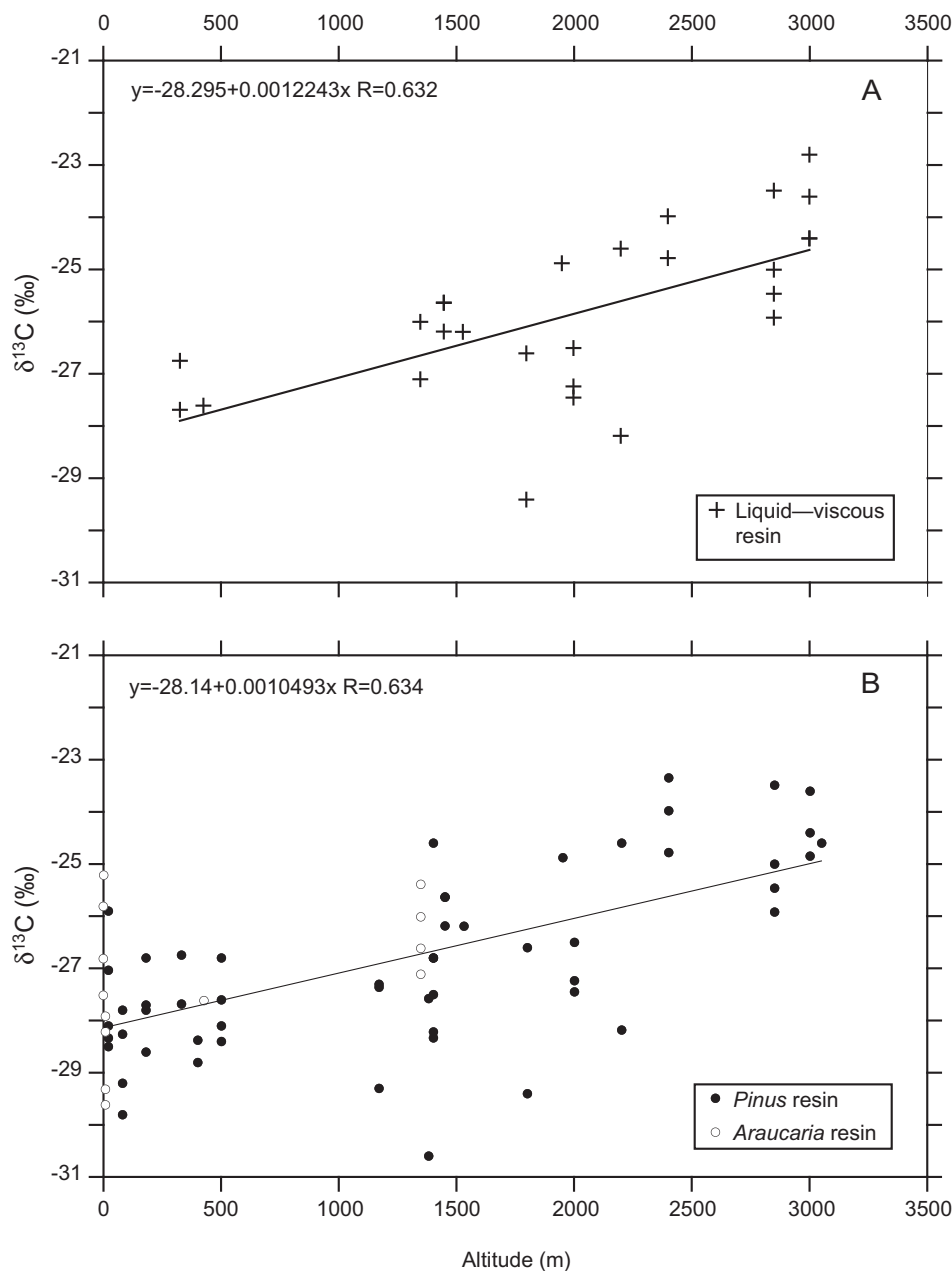
Fig. 4. Carbon-isotope data from modern *Pinus* and *Araucaria* resin plotted against altitude of the plant-growing site. (A) liquid–viscous resin samples, and (B) all resin samples.

($p = 0.001$) is observed between liquid–viscous (mean = −25.9‰) and solid resin (mean = −27.1‰), with an overall 1.2‰ ^{13}C-enriched values in the former (Fig. 3A). We conclude that volatile mono- and sesquiterpenes released by resin during hardening are more ^{13}C-enriched than the non-volatile diterpenoid and triterpenoid acids. Consequently, changes in the pristine $\delta^{13}C_{RESIN}$ occur soon after resin exudation. Future organic geochemical studies should precisely determine the magnitude of these isotopic changes in different resin types by studying the pattern of volatile loss during hardening, and the specific carbon-isotope signature and the relative abundance of the different resin compounds. Such a study would

probably allow correction of the measured $\delta^{13}C$ of solid resin back to the pristine signature at the time of exudation in order to faithfully interpret the data.

4.1.2. Differences between the $\delta^{13}C_{RESIN}$ and the $\delta^{13}C$ of other plant material

Post-photosynthetic fractionation in plants results in differences in the $\delta^{13}C$ of plant tissues (Badeck et al., 2005). In general, non-photosynthetic tissue tends to be more ^{13}C-enriched than photosynthetic tissue: leaves were found to have isotopically lighter values than wood and roots, and above-ground organs are more ^{13}C-depleted than below-ground material (Badeck et al., 2005;

Cernusak et al., 2009). Several biochemical causes have been invoked to explain this widespread isotopic behaviour

and are still a topic of debate (review by Cernusak et al., 2009).

$\Delta^{13}C_P$ during resin biosynthesis is evident from our data when comparing the $\delta^{13}C_{RESIN}$ with the $\delta^{13}C$ of other plant material. Our dataset shows that the mean $\delta^{13}C_{RESIN}$ of fresh liquid–viscous resin (−25.9‰) is more ^{13}C-enriched by 2.6‰ than the mean $\delta^{13}C_{LEAF}$ from a published compilation of data of C3 leaves (−28.5‰; Fig. 3A, Diefendorf et al., 2010), as expected from a non-photosynthetic plant compounds. Solid resin (−27.1‰) is more ^{13}C-depleted than liquid–viscous resin, but remains more ^{13}C-enriched than mean leaf $\delta^{13}C$, so that carbon-isotope changes due to hardening do not overshadow post-photosynthetic $\Delta^{13}C_P$ between resin and leaf. This difference is also evident from samples taken from the same trees and branches. Solid resin of *Araucaria heterophylla*, *Picea abies* and *Cupressus arizonica* sampled in the Botanical Garden in Padova (Italy) has higher $\delta^{13}C$ values than leaves from the same branch by approx. 1–2‰ (Fig. 3B and C). This difference should be corrected for the loss of volatiles and was likely larger by 1–2‰ at the time of resin exudation (see Section 4.1.1).

Similar differences exist also between resin and wood $\delta^{13}C$ signatures. In *Picea abies* and *Araucaria heterophylla*, resin is more ^{13}C-enriched than wood, which, in turn, shows very small $\delta^{13}C$ differences compared to leaf carbon-isotope signatures (Fig. 3B and C). As shown by the trees sampled for this study, fractionation during resin biosynthesis does occur and results in a very ^{13}C-enriched $\delta^{13}C_{RESIN}$ signature (by approx. 2–4‰) when compared to the $\delta^{13}C$ of other organs from the same plant branch. On the contrary, $\delta^{13}C_{WOOD}$ and $\delta^{13}C_{LEAF}$ show little difference (<1‰) within the same branch (Fig. 3B and C). Other studies show that on average stem wood and roots are more ^{13}C-enriched by 1–1.9‰ than is leaf material (Badeck et al., 2005). Our results suggest that the post-photosynthetic $\Delta^{13}C_P$ is larger for resin than for other bulk plant tissues. Such patterns are visible also after resin hardening, meaning that both volatile (monoterpenes and sesquiterpenes), and non-volatile (diterpene acids) are affected.

4.1.3. Environmental and physiological effects on $\delta^{13}C_{RESIN}$

Our results show that the carbon-isotope signature of resin records the environmental and physiological effects of C3 plant ^{13}C discrimination, as does other plant material. The $\delta^{13}C_{RESIN}$ varies by up to 2‰ within the same tree (Fig. 3C) and on average $\delta^{13}C_{RESIN}$ differs by up to 6‰ between plant species and genera, and between different localities (Table 1 and Supplementary Table 1). This high variability in the resin carbon-isotope composi-
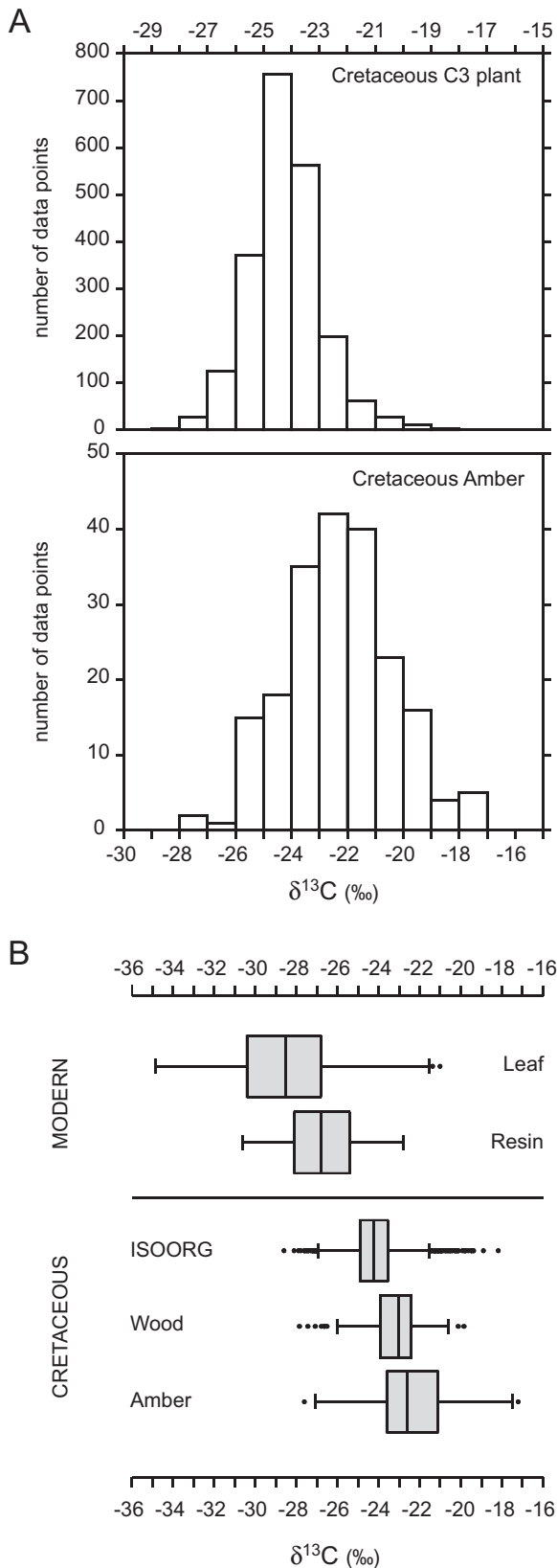
Fig. 5. (A) Comparison of the $\delta^{13}C$ data distribution of Cretaceous C3 plant material from the ISOORG database (Nordt et al., 2016) with amber. (B) Box-and-whiskers plots of $\delta^{13}C$ data of modern leaves (Diefendorf et al., 2010) and resin (this study), and Cretaceous ISOORG plants (Nordt et al., 2016), wood (Nordt et al., 2016; Salazar-Jaramillo et al., 2016) and amber (this study; Nissenbaum and Yakir, 1995; Dal Corso et al., 2013; Tappert et al., 2013).
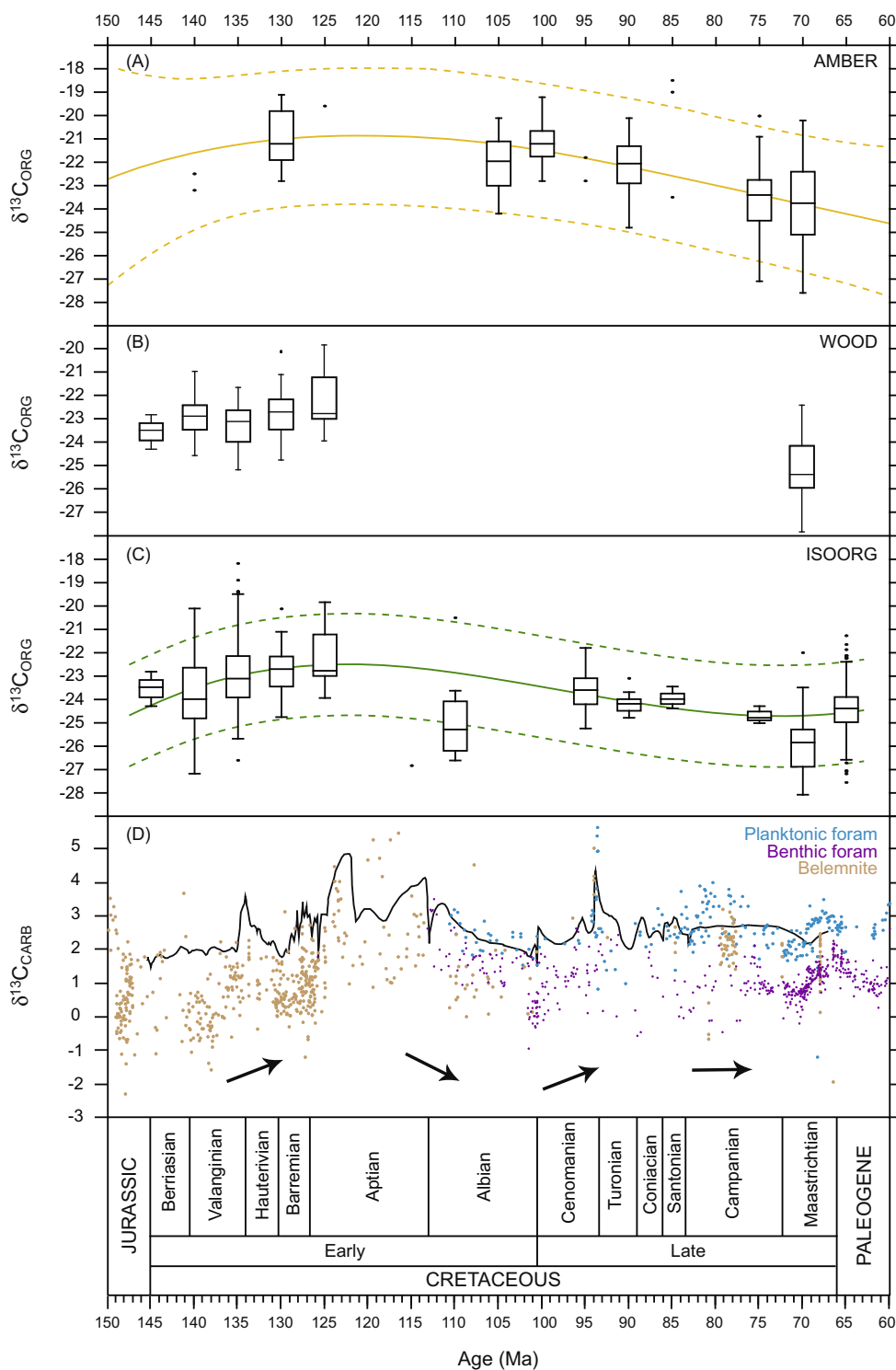
Fig. 6. Carbon-isotope (δ^{13}C) curves from Cretaceous amber, terrestrial organic matter, and marine carbonate. δ^{13}C data from plant material were grouped in 5 Myrs bins following the method used by Nordt et al. (2016) and a third-degree polynomial curve was fit to the plant data to highlight the main trends shown through the Cretaceous (see text for further explanation). (A) Compilation of Cretaceous amber carbon-isotope data from this study and Nissenbaum and Yakir (1995), Dal Corso et al. (2013) and Tappert et al. (2013). (B) Wood δ^{13}C data from Nordt et al. (2016) and Salazar-Jaramillo et al. (2016). (C) ISOORG δ^{13}C data from Nordt et al. (2016). ISOORG database comprises isotopic data from wood, leaf, charcoal, coal, palaeosols, and bulk terrestrial organic matter. (D) Marine carbonate carbon-isotope data from planktonic and benthic foraminifera, and belemnites (Prokoph et al., 2008 and Bodin et al., 2015). Whole-rock general carbonate curve (black line) replotted from Erba (2004). The arrows represent the main carbonate δ^{13}C trend during the Cretaceous. Time scale after Gradstein et al. (2012).
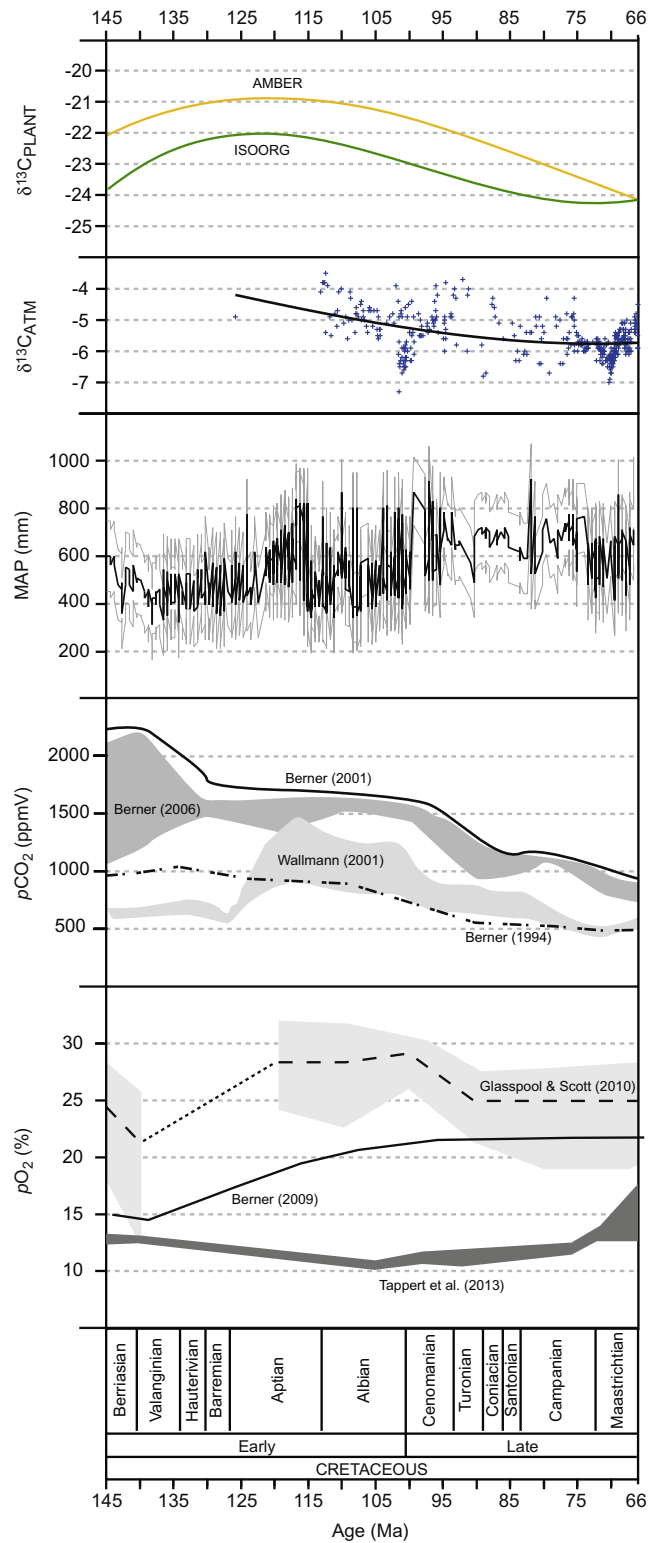
Fig. 7. Plant (amber and other plant material from the ISOORG database) $\delta^{13}C$ trends during the Cretaceous compared with the carbon-isotope composition of the atmosphere ($\delta^{13}C_{ATM}$) calculated from benthic foraminifera $\delta^{13}C$ and $\delta^{18}O$ (from Prokoph et al., 2008), the Mean Annual Precipitation (MAP) as reconstructed from compact-corrected depth to calcic horizon in palaeosols in the Colorado Plateau (Retallack, 2009), the pCO_2 calculated by different biogeochemical models (Berner, 1994, 2001, 2006; Wallmann, 2001; modified after Li et al., 2013), and the pO_2 inferred from charcoal abundance (Glasspool and Scott, 2010), biogeochemical modelling (Berner, 2009), and amber $\delta^{13}C$ (Tappert et al., 2013).

tion is likely related to the local climate and growing conditions, and plant physiology that regulate ^{13}C discrimination in plants [Eq. (1)].

Several studies have explored the dependence of plant ^{13}C discrimination in response to environmental gradients, which control the stomatal aperture and thus determine the c_i/c_a in [Eq. (1)] (see Cernusak et al., 2013 for a summary). As previously described, C3 plants fractionate carbon isotopes depending on a number of factors: mean annual precipitation, pCO_2, soil moisture, nutrient availability, irradiation, etc., can explain most of the $\delta^{13}C$ variability of plant biomass (e.g. Diefendorf et al., 2010; Kohn, 2010; Schubert and Jahren, 2012; Cernusak et al., 2013). Here we consider the variability of $\delta^{13}C_{RESIN}$ within the same tree, with changing altitude of the growing site and between plant species, and show that $\delta^{13}C_{RESIN}$ varies in ways that are similar to other plant material depending on the environmental conditions under which the plant grew.

Solid resin $\delta^{13}C$ varies within an individual *Araucaria heterophylla* by approx. 2‰ (depending on different heights along the trunk), as also observed for leaf and wood $\delta^{13}C$ (Fig. 3C). This difference suggests that either seasonality and/or physiological factors can considerably change the $\delta^{13}C_{RESIN}$ within an individual plant. This phenomenon has also been observed in leaf $\delta^{13}C$, which varies by approx. 1–4‰ along vertical canopy profiles in conifers (e.g. Duursma and Marshall, 2006 and references therein). $\delta^{13}C_{LEAF}$ generally increases from the bottom to the top of the crown due to hydraulic conductance or irradiation variations (Koch et al., 2004; Duursma and Marshall, 2006; Cernusak et al., 2013). Our resin, leaf and wood $\delta^{13}C$ data from *Araucaria heterophylla* appear to show a similar pattern (Fig. 3C).

The $\delta^{13}C$ of fresh liquid–viscous resin (Fig. 4A) increases with altitude from sea level to 3050 m (Fig. 4B). This effect is also evident when plotting solid and liquid–viscous resin of *Pinus* and *Araucaria*, the most representative genera. In both cases $\delta^{13}C_{RESIN}$ increases linearly with altitude ($p < 0.001$; Fig. 4). These results contradict a previous study on $\delta^{13}C_{RESIN}$, which found a general ^{13}C-depletion along altitudinal transects in the UK to a maximum altitude of 550 m (Stern et al., 2008). The dataset of $\delta^{13}C_{RESIN}$ values presented in this study comprises a sample from altitudes up to approx. 3000 m and is more comparable to the existing $\delta^{13}C$ data from C3 leaves and wood from localities around the world of altitudes up to 5600 m (Körner et al., 1988; Warren et al., 2001). Decreasing ^{13}C discrimination with altitude has been extensively observed in conifer leaves and wood (e.g. Körner et al., 1988, 1991; Hultine and Marshall, 2000; Warren et al., 2001; Cernusak et al., 2013). The net effect of altitude on plant $\delta^{13}C$ is, however, considered negligible compared, for example, to the MAP (Kohn, 2016). Indeed, the mechanism by which the discrimination-altitude correlation operates is unclear: many authors have invoked changes in leaf morphology, water availability, leaf nitrogen content, temperature, decrease of pCO_2 with elevation, pO_2 and irradiance as pos-

sible causes (e.g. Hultine and Marshall, 2000; Diefendorf et al., 2010; Cernusak et al., 2013). The strong dependence of plant $\delta^{13}C$ towards very different environmental factors (e.g. Arens et al., 2000; Diefendorf et al., 2010) points to a possible combined effect of these factors on $\delta^{13}C_{RESIN}$ with altitude. Additional $\delta^{13}C_{RESIN}$ analyses along altitudinal transects coupled with precise data about the environmental conditions (moisture levels, temperature, irradiance, etc.) will elucidate the $\delta^{13}C_{RESIN}$-altitude correlation found in this study and permit a greater understanding of the relative contribution of these effects on the final carbon-isotope signature of the resin. The significant correlation between $\delta^{13}C_{RESIN}$ and altitude, which is similar to the correlation found using other plant material, means that environmental effects on $\Delta^{13}C_P$ are recorded by resin despite fractionation during biosynthesis, which determines the differences between its $\delta^{13}C$ and that of other tissues (Fig. 3B and C), and during hardening (Fig. 3).

Several authors have reported high $\delta^{13}C$ variability (e.g. up to 6‰ in lowland rainforest stands; Bonal et al., 2000) among plant species under the same environmental conditions (e.g. Leavitt and Long, 1986; Zhang and Cregg, 1996; Cui and Schubert, 2016 and references therein). These inter-specific differences in the $\delta^{13}C$ of plants are related to differences in $\Delta^{13}C_P$ regulated by the morphology of leaf and stomata that control efficiency of water use and the c_i/c_a ratio (Murray et al., 1998). The $\delta^{13}C$ of resins sampled at the same altitude in the same locality (Padova, Italy) from different tree genera differs by about 2–5‰ (Fig. 3B). Overall, the $\delta^{13}C_{RESIN}$ varies by up to 6‰ between plant species (Table 1). These findings suggest that variations in ^{13}C discrimination linked to plant physiology are recorded also by resin. Interestingly, when resin data are grouped at a high taxonomic level, the $\delta^{13}C$ differences are not statistically significant ($p = 0.598$) and their mean calculated $\delta^{13}C_{RESIN}$ values (*Araucaria* = −27.1‰; *Pinus* = −26.9‰) approach that of the mean of our worldwide resin samples.

4.2. Cretaceous $\delta^{13}C_{AMBER}$ data

As hypothesized in the introduction, amber could potentially be used to reconstruct the carbon-isotope composition of the palaeoatmosphere, as is the case with leaf and wood. Our data on modern material show that the $\delta^{13}C_{RESIN}$ can record changes in ^{13}C discrimination by C3 plants as seen in leaves and wood. Records of the $\delta^{13}C$ from fossil wood and bulk leaves or cuticles, despite their natural variability within each stratigraphic interval, parallel those of marine carbonates and can record global long- and short-term perturbations of the carbon cycle (e.g. Gröcke et al., 1999; Gröcke, 2002; Dal Corso et al., 2011). It is therefore reasonable to expect amber to record the same carbon-isotope changes. In the following sections we will discuss the potential of amber as a chemostratigraphic tool and as a proxy for Cretaceous palaeoatmosphere in the light of present-day resin carbon-isotope geochemistry.

4.2.1. Carbon-isotope signature of Cretaceous amber vs other C3 fossil plant material: pristine differences and diagenetic effects

On average, Cretaceous $\delta^{13}C_{AMBER}$ (mean = −22.3‰ ± 1.9‰) is ^{13}C-enriched by 1.6‰ ($p < 0.0001$) relative to other C3 plant material (mean = −24.2‰ ± 1.3‰) and wood (mean = −23.1‰ ± 1.3‰) (Fig. 5). Amber is always more ^{13}C-enriched than wood by 1.5–2‰ for each age bin present here (Table 2, Fig. 6). A similar offset was also observed for Upper Triassic conifer amber and wood from Italy (+2.5‰) (Dal Corso et al., 2011), and for Upper Cretaceous gymnosperm-derived coals and associated resinites from Australia (+2.6‰) (Murray et al., 1998). A recent compilation of plant $\delta^{13}C$ data for all the Phanerozoic shows amber is on average the most ^{13}C-enriched plant tissue (Nordt et al., 2016). The differences between resin and plant tissues (leaf and wood) observed in our modern material (Fig. 3) can explain amber ^{13}C-enriched values, showing that fossil material can retain the same patterns observed in modern samples, that is, with the differences being generated by fractionation during resin biosynthesis. Moreover, the dispersion of $\delta^{13}C$ data is larger in amber (SD = 1.95‰; IQR = 2.5‰) than in other C3 plant material (SD = 1.31‰; IQR = 1.4‰) (Table 2). This difference is evident also when considering separately different plant material with a sample size similar to the size of our amber database and with the same age. In general, amber $\delta^{13}C$ values are more scattered than those of Cretaceous wood (SD = 1.31‰; IQR = 1.47‰), charcoal (SD = 1.55‰; IQR = 2‰) and coal (SD = 1.43‰; IQR = 1.23‰). In the Hauterivian–Barremian (age bin = 130 Ma) and Maastrichtian (age bin = 70 Ma) $\delta^{13}C_{AMBER}$ has a greater spread in values than wood $\delta^{13}C$; and in the Turonian (90 Ma) and in the Maastrichtian (70 Ma) the amber carbon-isotope signature is more variable than in other plant substrates (Fig. 6; Table 2).

Comparison with modern material (Fig. 5B) shows that amber record an original high plant $\delta^{13}C$ variability, contrary to other fossil plant remains (see also Dal Corso et al., 2011). Taphonomical and diagenetic processes could enhance the original $\delta^{13}C$ discrepancies between plant material and accentuate the spread in $\delta^{13}C$ data. The carbon-isotope signature of plant tissue changes towards more negative values during diagenesis (Spiker and Hatcher, 1987), a fact also confirmed here for conifer resin (Fig. 3A). As previously discussed (Section 4.1.2), solid resin becomes more depleted by 1.2‰ when altered from fresh liquid–viscous resin, probably because of the loss of ^{13}C-rich volatiles during hardening (Fig. 3A). Subsequently, resin maturation causes polymerization of non-volatile components accompanied by cross-linking and isomerization, but no significant diagenetic changes of the carbon-isotope composition take place (Dal Corso et al., 2013; Tappert et al., 2013). In support of this assumption, Dal Corso et al. (2013) observed that altered and unaltered areas within the same Lower Cretaceous amber pieces from the San Just deposit show no $\delta^{13}C$ differences despite oxidation and degradation, as revealed by infra-red spectroscopic and thermogravimetric analyses. This observation indicates that amber is a closed system with respect to carbon-isotopes as soon as it hardens. By contrast, other plant remains can experience a more pervasive diagenetic overprint. Charcoalification and coalification can severely change the pristine $\delta^{13}C$ of tissues (e.g. Gröcke, 1998; Yans et al., 2010 and references therein). Pyrolysis experiments have shown the $\delta^{13}C$ of wood to become either more ^{13}C-enriched or depleted depending on the temperature of combustion reached (Jones and Chaloner, 1991; Hall et al., 2008). Upon burial, the preferential degradation of hemicellulose (average $\delta^{13}C$ of about −23‰) and cellulose (average $\delta^{13}C$ of about −25‰) over lignin (average $\delta^{13}C$ of about −28‰) can change the pristine bulk wood $\delta^{13}C$ by several ‰ towards more negative values (e.g. Spiker and Hatcher, 1987; van Bergen and Poole, 2002). As pointed out by Dal Corso et al. (2011), these diagenetic processes could be responsible not only for changing the average $\delta^{13}C$ of plant tissue but also for narrowing $\delta^{13}C$ variability of Triassic fossil wood and leaves compared with amber. Similarly, the Cretaceous $\delta^{13}C_{AMBER}$ is consistently more variable than the $\delta^{13}C$ of other plant substrates (Figs. 5 and 6, Table 2). Despite these complicating factors, data confirm that amber is very resistant to diagenesis and can preserve the pristine carbon-isotope signature of resin better than other plant material and, consequently, can retain information about past environments and climate.

4.2.2. Interpreting $\delta^{13}C_{AMBER}$ record through the Cretaceous and comparison with terrestrial organic matter and marine carbonate carbon-isotope records

Excluding the Barriasian–Valanginian interval for which the $\delta^{13}C_{AMBER}$ data available are indeed very scarce, the most remarkable feature shown by the Cretaceous $\delta^{13}C_{AMBER}$ record is an approximately 2.5‰ negative trend from the Hauterivian–Barremian (130 Ma) to the Maastrichtian (70 Ma). Similarly, Late Cretaceous wood $\delta^{13}C$ is more ^{13}C-depleted than Early Cretaceous wood $\delta^{13}C$ (Fig. 6). Maastrichtian C3 plant $\delta^{13}C$ data from ISOORG compiled by Nordt et al., 2016 (various types of fossil C3 plant remains minus amber data) are approximately 3‰ more ^{13}C-depleted than the Hauterivian–Barremian $\delta^{13}C$ data (Fig. 6). In the earliest Cretaceous, ISOORG $\delta^{13}C$ rises from the Jurassic–Cretaceous boundary to the early Albian (125 Ma). The $\delta^{13}C$ changes shown by ISOORG, wood, and amber records during the Cretaceous are very similar to or smaller than their carbon-isotope variability within each age bin (Table 2 and Fig. 6). Moreover, the resolution of the data is very low and long intervals of the Cretaceous are not covered. This drawback obviously hampers a correct interpretation of the trends because the non-homogeneous distribution of data through time biases the fitting. However, the overall 2.5–3‰ negative depletion towards the end of the Cretaceous is in clear agreement among the global compilation of plant substrates. On the contrary, the marine carbonate carbon-isotope records seem only to partially parallel the terrestrial long-term signal. In the Early Cretaceous belemnite $\delta^{13}C$ record, a long-term positive trend from the late Berriasian–early Valanginian to the middle Aptian is followed by a long-term negative trend, which ends in the middle Albian (Prokoph et al., 2008; Bodin et al., 2015). For subsequent intervals, belem-

nite $\delta^{13}C$ data are sparse but become overall more ^{13}C-enriched in the Late Cretaceous (Fig. 6). Data from planktonic and benthic foraminifera are available only from the early Albian onwards: $\delta^{13}C$ declines by approx. 1‰ from the early Albian to the Albian–Cenomanian boundary, then rises by the same magnitude until the Cenomanian–Turonian boundary and remains stable until the end of the Cretaceous (Fig. 6; Prokoph et al., 2008). The schematic curve of whole-rock carbonate $\delta^{13}C$ analyses compiled by Erba (2004) mirrors the belemnite and foraminiferal records (Fig. 6). Despite the offset in the carbon-isotope signature of the different proxies, which depends on the water mass in which the carbonate was precipitated or secreted (Prokoph et al., 2008), marine carbonates show the same general carbon-isotope trends during the Cretaceous (Fig. 6). Using the equation proposed by Tipple et al. (2010), we calculated the $\delta^{13}C$ of the Cretaceous atmosphere ($\delta^{13}C_{ATM}$) from the available $\delta^{13}C$ data of benthic foraminifera compiled by Prokoph et al. (2008). The polynomial curve fitted to the inferred $\delta^{13}C_{ATM}$ data points shows a small long-term decline from approx. 125 Ma to the end of the Cretaceous (Fig. 7). The $\delta^{13}C_{ATM}$ trend seems to mimic the 2.5–3‰ negative trend described by C3 plant material, although with a much smaller magnitude (1‰) (Fig. 7). This general relationship suggests that $\delta^{13}C$ from Cretaceous amber and other plant tissues, despite high variability within each age bin, can record changes in the carbon-isotope composition of the atmosphere. The relatively small atmospheric shift, however, cannot alone explain alone the changes in plant $\delta^{13}C$ records. These data also suggest $\Delta^{13}C_P$ increased towards the end of the Cretaceous along with decreasing $\delta^{13}C_{ATM}$ values. It is thus necessary to account for changes in climate and floral community structure, upon which $\Delta^{13}C_P$ is strongly dependent, to faithfully interpret Cretaceous plant $\delta^{13}C$ data (e.g. Diefendorf et al., 2010; Schubert and Jahren, 2013).

Given the different provenances of Cretaceous amber, some of the changes in its $\delta^{13}C$ through time and the large variability within each age bin (Fig. 6) can be attributed to local plant growing conditions, which are hardly constrainable for amber deposits, given the fact that amber is rarely found *in situ* but is mostly reworked. The altitude of the Cretaceous resin-producing trees, seemingly an important control on modern resin carbon-isotope signature (see Section 3), is relatively well known for those examples situated close to former sea level, namely the Albian amber deposits (Peñacerrada, El Soplao), Albian-Cenomanian amber deposits (Archingeay-Les Nouillers, Cadeuil, Fouras, Ile d'Aix, La Buzinie: Girard et al., 2008; Néraudeau et al., 2009) and the Santonian amber deposits (Belcodène, Piolenc: Gomez et al., 2003; Saint-Martin et al., 2013). However, for other deposits the palaeo-altitude is unknown and presumably variable. The depleted $\delta^{13}C$ values of Campanian amber from Canada could be partially related to a particularly high palaeo-latitudinal location of the deposits (Fig. 1) and possibly from a different climatic regime (see compilation by Scotese, 2002). Insect infestation has been shown to have substantially ^{13}C-enriched the $\delta^{13}C$ of part of the Turonian New Jersey ambers analysed by McKellar et al. (2011), which are also included in our data-

set (Fig. 6). At a micro-environmental scale, the height at which the Cretaceous amber was produced within the tree trunk is impossible to determine, and this factor has been previously shown to affect the $\delta^{13}C$ of modern resin by several ‰ (see Section 3). Different fractionation pathways of different plant functional types through time could also be responsible for the $\delta^{13}C_{AMBER}$ changes (Diefendorf et al., 2010). In fact, the species composition responsible for the amber production differed through the Cretaceous, even though the number of species remained the same (1–2) for each time interval (see, e.g., Tappert et al., 2013; Nohra et al., 2015). As previously described, modern $\delta^{13}C_{RESIN}$ varies by up to 6‰ between plant species from different localities (Table 1), and the $\delta^{13}C$ of resins sampled in the same locality from different tree species differs by about 2–5‰ (Fig. 3B). To avoid this problem it is recommended to use a plant substrate that averages the inter-specific carbon-isotope differences for palaeo-atmosphere reconstructions (e.g. Arens et al., 2000).

Significantly, the Cretaceous Period was a time of rapid taxonomic diversification and ecological radiation of angiosperms, starting from the Aptian–Albian and continuing to the Campanian (McElwain et al., 2005). Angiosperm tissue $\delta^{13}C$ is generally more depleted than conifer tissue $\delta^{13}C$ (Arens et al., 2000; Diefendorf et al., 2010), something reflected in the isotopic composition of modern resin (Murray et al., 1998). The decline in the carbon-isotope composition of plant material, of which the botanical affinity is unknown, from the Early to the latest Cretaceous (Fig. 6) could be related to an increase in the relative abundance of Angiosperms. This factor could lie behind the ISOORG trends, where tissues from different sources are grouped together (charcoal, coal, leaf, wood and bulk terrestrial organic matter), but Cretaceous amber considered in this study comes only from conifers (e.g. Tappert et al., 2013). Therefore, micro-environmental conditions, different plant functional type discrimination, and diagenesis (see Section 4.2.1) are all factors that could have modified the Cretaceous plant $\delta^{13}C$ signature and determined the high variability for each age bin, but such factors are difficult to constrain for the fossil record and thus their relative effect on plant $\delta^{13}C$ cannot be calculated. However, the similar general long-term $\delta^{13}C$ patterns shown by ISOORG, wood, and amber suggest there is a global dominant factor that regulated plant discrimination throughout the long time scale of the Cretaceous (from 145 Ma to 66 Ma; Gradstein et al., 2012).

Today, MAP accounts for more than the 50% of the variations observed in $\Delta^{13}C_P$, implying that stomatal conductance (c_i/c_a in Eq. (1)) is primarily driven by water availability: The $\Delta^{13}C_P$ increases with increasing MAP (Diefendorf et al., 2010; Kohn, 2010). Diefendorf et al. (2015) showed that $\Delta^{13}C_P$ in Palaeogene plants responded to water availability in a way similar to modern plants. MAP calculated from compact-corrected depth to calcic horizon in palaeosols in the Colorado Plateau (Retallack, 2009) indicates Late Cretaceous MAP was higher (approx. 600–650 mm on average) than the Early Cretaceous MAP (approx. 450 mm on average) in the study area (Fig. 7). According to the general $\Delta^{13}C_P$–MAP relationship

calculated for modern leaves (Diefendorf et al., 2010), such increase of MAP would increase the $\Delta^{13}C_P$ by approx. 1–2‰. Consequently, the plant carbon-isotope composition would become more ^{13}C-depleted, suggesting that Cretaceous plant $\delta^{13}C$ data record changes in the global hydrological cycle, as predicted by the relationships found by Diefendorf et al. (2010) and Kohn (2010) for modern leaf $\delta^{13}C$. Calculation of Cretaceous MAP from $\delta^{13}C_P$ compilations using the proposed relationships is not possible. Information to compute the data (plant functional type, altitude and latitude of growing site) is either missing or very vague, and the plant substrate is mixed, i.e. derives from different plant material (amber, wood, charcoal, coal, leaf, bulk terrestrial organic matter) for which the botanical affinity is largely unknown.

Schubert and Jahren (2012) found a strong relationship between $\Delta^{13}C_P$ and pCO_2 for plants grown in chambers with controlled environmental conditions. According to their model, $\Delta^{13}C_P$ hyperbolically increases with increasing pCO_2 levels. This relationship was validated against ice-core pCO_2 data for the Last Glacial Maximum and used to reconstruct the pCO_2 at the Palaeocene–Eocene Thermal maximum (Schubert and Jahren, 2013, 2015). In contrast to these studies, Cretaceous $\delta^{13}C_{AMBER}$ and $\delta^{13}C_{ISOORG}$ show the most ^{13}C-enriched values in intervals of predicted high pCO_2 and the most ^{13}C-depleted values in intervals of predicted low pCO_2 (Fig. 7, see also Wang et al., 2014), as also previously noted by Tappert et al. (2013). Precise calculation of $\Delta^{13}C_P$ is not possible for our dataset, given the age uncertainties of the samples and thus the difficulty in assigning to each $\delta^{13}C_P$ data point a precise value of $\delta^{13}C_{ATM}$. However, as previously described, comparison of the magnitude of the long-term negative trend of $\delta^{13}C_{ATM}$ with the magnitude of amber and similar ISOORG $\delta^{13}C$ trend suggests that $\Delta^{13}C_P$ increased in the Late Cretaceous. This result suggests that either pCO_2 has no effect on plant $\delta^{13}C$ during the Cretaceous or that the pCO_2 reconstructions made via biogeochemical modelling are incorrect. Similar to what was found in this study, Diefendorf et al. (2015) found that $\Delta^{13}C_P$ does not increase in correspondence with intervals of high pCO_2 in the Palaeogene. Kohn (2016) found no or negligible pCO_2 dependence of $\delta^{13}C_P$ in selected Cenozoic case studies. This phenomenon is explained by the ability of plants to evolve within decadal–centurial timescales in response to changing pCO_2 by adjusting their physiology to maintain an ideal c_i/c_a ratio (Diefendorf et al., 2015; Kohn, 2016 and references therein). By contrast, on shorter timescales (<1 year chamber growth experiments), plants respond to changing pCO_2 through the stomata, thus changing the c_i/c_a (Eq. (1); Diefendorf et al., 2015).

The $\delta^{13}C$ of amber and plant tissues seems to decrease with increasing pO_2 levels, as independently inferred by biogeochemical modelling (Berner, 2009) and charcoal abundance (Glasspool and Scott, 2010) (Fig. 7). Such a relationship is in line with theoretical expectations and the results obtained in controlled chamber experiments, which show $\Delta^{13}C_P$ increases by 1.5–3.5‰ in high (35%) pO_2 (Berner et al., 2000; Beerling et al., 2002). As previously mentioned, Tappert et al. (2013) proposed the use of

$\delta^{13}C_{AMBER}$ to reconstruct palaeo-pO_2, assuming that, at ambient air, the $\Delta^{13}C_P$ is proportional to pO_2 and that physiological adaptations did not occur through time. The Cretaceous pO_2 model proposed by Tappert et al. (2013) fails to reproduce the pO_2 trends calculated by other authors (Fig. 7) and contradicts plant $\delta^{13}C$ data compiled in this study. This difference could be related to the difficulty in calculating past $\delta^{13}C_{ATM}$ and the use of mean $\delta^{13}C_{AMBER}$, which are terms in the equations proposed by Tappert et al. (2013) to infer pO_2 from $\delta^{13}C_{AMBER}$. Indeed, small variations in growing conditions, such as light exposure, nutrient, and water levels, can mask the pO_2 effect on plant $\delta^{13}C$, as shown during controlled chamber experiments (Beerling et al., 2002). Therefore, accurate reconstruction of past atmospheric pO_2 from mean $\delta^{13}C$ of ambers is fraught with difficulties, given that the $\delta^{13}C$ of resin varies enormously, even at the scale of a single tree (see Section 3). Moreover, Tappert et al. (2013) assumed in their model that physiological adaptations did not occur but, as discussed above, on long timescales plants do evolve to maintain an ideal leaf–gas exchange optimum. The observed correspondence between biogeochemical modelling and charcoal pO_2 records and $\delta^{13}C_P$ (both amber and other plant material) points to a possible pO_2 effect on Cretaceous C3 $\Delta^{13}C_P$ that definitely deserves further exploration.

5. CONCLUSIONS

Our carbon-isotope analysis of modern conifer resin and associated plant tissues showed that hardening after exudation causes an overall ^{13}C-enrichment in the bulk carbon-isotope signature of resin. This process is evident comparing the $\delta^{13}C$ of liquid–viscous (mean = −25.9‰) to the $\delta^{13}C$ of solid resins (mean = −27.1‰) and is explained by selective loss of ^{13}C-depleted volatiles. Carbon-isotope fractionation during resin biosynthesis occurs and results in a more ^{13}C-enriched $\delta^{13}C_{RESIN}$ signature (by approx. 2–4‰) than the $\delta^{13}C$ of other material sampled from the same plant branch. By contrast, wood and leaf $\delta^{13}C$ show little difference (<1‰) within the same branch. The results of this study suggest post-photosynthetic $\Delta^{13}C_P$ is larger in resin than in other plant material. Furthermore, the variability of the $\delta^{13}C_{RESIN}$ is high (approx. 8‰), ranging from −30.6‰ to −22.8‰. $\delta^{13}C_{RESIN}$ shows differences of up to 6‰ between plant species, locality and within a single tree. $\delta^{13}C_{RESIN}$ of different tree genera growing in the same locality and at the same altitude shows differences of about 2–5‰ $\delta^{13}C_{RESIN}$. $\delta^{13}C_{RESIN}$ becomes more ^{13}C-enriched with increasing altitude. The environmental variability of $\delta^{13}C$ of resin is similar to that reported for leaf and wood, suggesting the potential to record changes in $\Delta^{13}C_P$ by C3 plants. Therefore, resin appears to be a valuable proxy for carbon-isotope studies in modern plant ecology and physiology.

Our meta-analysis of new and published Cretaceous $\delta^{13}C_P$ (amber, wood and mixed material) revealed that Cretaceous $\delta^{13}C_{AMBER}$ (mean = −22.3‰ ± 1.9‰) is more ^{13}C-enriched than other Cretaceous C3 plant material $\delta^{13}C$ (mean = −24.2‰ ± 1.3‰) and wood (mean = −23.1‰

$\pm$ 1.3‰), as observed in modern plants. Therefore, we conclude that fossil material can retain the same patterns observed in modern samples, i.e. the differences being generated by $\Delta^{13}C_P$ during resin biosynthesis. In the Cretaceous, $\delta^{13}C_{AMBER}$ has variability similar to modern resin, but the scatter of $\delta^{13}C_{AMBER}$ data is larger than the scatter of $\delta^{13}C$ data of other fossil C3 plant material, which is attributed to diagenesis. Amber has been shown to become a closed system with respect to carbon isotopes soon after hardening, whereas other plant remains can experience a more pervasive diagenetic overprint (both ^{13}C enrichment or depletion). Diagenetic processes could be responsible also for narrowing $\delta^{13}C$ variability by selectively removing specific compounds such as volatiles. These observations suggest amber can preserve the pristine $\delta^{13}C$ signature better than other plant material and, consequently, the original high $\delta^{13}C$ variability as shown by modern plants. Thus, amber can retain faithful information about past environments and climate.

Despite the large variability, amber, wood, and mixed plant tissue (ISOORG) record similar long-term trends during the Cretaceous. In particular, plant material record a 2.5–3‰ negative trend from the Hauterivian–Barremian to the Maastrichtian that mirrors a similar but smaller (1‰) shift in the $\delta^{13}C$ of the atmosphere calculated from benthic foraminifera $\delta^{13}C$ and $\delta^{18}O$ data compilation. Increasing mean annual precipitation and/or pO_2 levels could have increased $\Delta^{13}C$ of plants during the Cretaceous, thus increasing the magnitude of the negative trend. Comparing the isotopic records with pCO_2 trends suggests that pCO_2 did not affect $\Delta^{13}C_P$ on the long-time scale considered in this study.

Our study thus shows that in the deep past the interpretation of the $\delta^{13}C_{AMBER}$ curve and, by extension, the $\delta^{13}C$ of terrestrial plants is ambiguous to some extent due to the difficulty in constraining the environmental and physiological factors that control the natural variability of $\delta^{13}C_{RESIN}$ and due to the uncertainties in determining the precise age of some of the analysed material. However, meta-analysis of marine and terrestrial $\delta^{13}C$ records coupled to the amber record reveals isotopic variations that seem ascribable to changes in the composition of the Cretaceous atmosphere–ocean system and climate. Improvement of the resolution of the existing data and collection of information about botanical source and environmental growing conditions of the fossil plant material will undoubtedly improve our understanding of amber $\delta^{13}C$ records and allow more faithful reconstruction of the past atmosphere.

APPENDIX A. SUPPLEMENTARY DATA

Supplementary data associated with this article can be found, in the online version, at http://dx.doi.org/10.1016/j.gca.2016.11.025.

REFERENCES

Aquilina L., Girard V., Henin O., Bouhnik-Le Coz M., Vilbert D., Perrichot V. and Néraudeau D. (2013) Amber inorganic geochemistry: new insights into the environmental processes in a Cretaceous forest of France. *Palaeogeogr. Palaeoclimatol. Palaeoecol.* **369**, 220–227.

Arens N. C., Jahren A. H. and Amundson R. (2000) Can C3 plants faithfully record the carbon isotopic composition of atmospheric dioxide?. *Paleobiology* **26** 137–164.

Badeck F. W., Tcherkez G., Nogues S., Piel C. and Ghashghaie J. (2005) Post-photosynthetic fractionation of stable carbon isotopes between plant organs - a widespread phenomenon. *Rapid Commun. Mass Spectrom.* **19**, 1381–1391.

Barrón E., Peyrot D., Rodríguez-López J. P., Meléndez N., López-del Valle R., Najarro M., Rosales I. and Comas-Rengifo M. J. (2015) Palynology of Aptian and upper Albian (Lower Cretaceous) amber-bearing outcrops of the southern margin of the Basque-Cantabrian basin (northern Spain). *Cretac. Res.* **52**, 292–312.

Batten D., Colin J. P. and Néraudeau D. (2010) Megaspores from mid Cretaceous deposits in western France and their biostratigraphic and palaeoenvironmental significance. *Rev. Palaeobot. Palynol.* **161**, 151–167.

Bechtel A., Sachsenhofer R. F., Gratzer R., Lucke A. and Puttmann W. (2002) Parameters determining the carbon isotopic composition of coal and wood in the Early Miocene Oberdorf lignite seam (Styrian Basin, Austria). *Org. Geochem.* **33**, 1001–1024.

Bechtel A., Gratzer R., Sachsenhofer R. F., Gusterhuber J., Lucke A. and Puttmann W. (2008) Biomarker and carbon isotope variation in coal and fossil wood of Central Europe through the Cenozoic. *Palaeogeogr. Palaeoclimatol. Palaeoecol.* **226**, 166–175.

Beerling D. J., Lake J. A., Berner R. A., Hickley L. J., Taylor D. W. and Royer D. L. (2002) Carbon isotope evidence implying high O_2/CO_2 ratios in the Permo-Carboniferous atmosphere. *Geochim. Cosmochim. Acta* **66**, 3757–3767.

Berner R. A. (1994) GEOCARB II: a revised model of atmospheric CO_2 over Phanerozoic time. *Am. J. Sci.* **294**, 56–91.

Berner R. A. (2001) Modelling atmospheric O_2 over Phanerozoic time. *Geochim. Cosmochim. Acta* **65**, 685–694.

Berner R. A. (2006) Inclusion of the weathering of volcanic rocks in the GEOCARBSULF model. *Am. J. Sci.* **306**, 295–302.

Berner R. A. (2009) Phanerozoic atmospheric oxygen: new results using the GEOCARBSULF model. *Am. J. Sci.* **309**, 603–606.

Berner R. A., Petsch S. T., Lake J. A., Beerling D. J., Popp B. N., Lane R. S., Laws E. A., Westley M. B., Cassar N., Woodward F. I. and Quick W. P. (2000) Isotope fractionation and atmospheric oxygen: implications for Phanerozoic O_2 evolution. *Science* **287**, 1630–1633.

Bodin S., Meissner P., Janssen N. M. M., Steuber T. and Mutterlose J. (2015) Large igneous provinces and organic carbon burial: controls on global temperature and continental weathering during the Early Cretaceous. *Global Planet. Change* **133**, 238–253.

Bonal D., Sabatier D., Montpied P., Tremeaux D. and Guehl J. M. (2000) Interspecific variability of d13C among trees in rainforest of French Guiana: functional groups and canopy integration. *Oecologia* **124**, 454–468.

Cerling T. E. and Harris J. M. (1999) Carbon isotope fractionation between diet and bioapatite in ungulate mammals and implications for ecological and paleoecological studies. *Oecologia* **120**, 347–363.

Cernusak L. A., Tcherkez G., Keitel C., Cornwell W. K., Santiago L. S., Knohl A., Barbour M. M., Williams D. G., Reich P. B., Ellsworth D. S., Dawson T. E., Griffiths H. G., Farquhar G. D. and Wright I. J. (2009) Why are non-photosynthetic tissues generally ^{13}C enriched compared with leaves in C_3 plants? Review and synthesis of current hypotheses. *Funct. Plant Biol.* **36**, 199–213.

Cernusak L. A., Ubierna N., Winter K., Holtum J. A. M., Marshall J. D. and Farquhar G. D. (2013) Environmental and physiological determinants of carbon isotope discrimination in terrestrial plants. *New Phytol.* **200**, 950–965.

Coplen T. B., Brand W. A., Gehre M., Gröning M., Meijer H. A. J., Toman B. and Verkouteren R. M. (2006) New Guidelines for [13]C Measurements. *Anal. Chem.* **78**(7), 2439–2441.

Cui Y. and Schubert B. A. (2016) Quantifying uncertainty of past pCO2 determined from changes in C3 plant carbon isotope fractionation. *Geochim. Cosmochim. Acta* **172**, 127–138.

Dal Corso J., Preto N., Kustatscher E., Mietto P., Roghi G. and Jenkyns H. (2011) Carbon-isotope variability of Triassic amber, as compared with wood and leaves (Southern Alps, Italy). *Palaeogeography, Palaeclimatology, Palaeoecology* **302**, 187–193.

Dal Corso J., Roghi G., Ragazzi E., Angelini I., Giaretta A., Soriano C., Delclòs X. and Jenkyns H. C. (2013) Physicochemical analysis of Albian (Lower Cretaceous) amber from San Just (Spain): implications for palaeoenvironmental and palaeoecological studies. *Geologica Acta* **11**, 359–370.

Diefendorf A. F., Mueller K. E., Wing S. L., Koch P. L. and Freeman K. H. (2010) Global patterns in leaf ^{13}C discrimination and implications for the studies of past and future climate. *Proc. Natl. Acad. Sci.* **107**, 5738–5743.

Diefendorf A. F., Freeman K. H., Wing S. L., Currano E. D. and Mueller K. E. (2015) Paleogene plants fractionated carbon isotope similar to modern plants. *Earth Planet. Sci. Lett.* **429**, 33–44.

Duursma R. A. and Marshall J. D. (2006) Vertical canopy gradients in d13C correspond with leaf nitrogen content in a mixed-species conifer forest. *Trees* **20**, 496–506.

Erba E. (2004) Calcareous nannofossils and Mesozoic oceanic anoxic events. *Mar. Micropaleontol.* **52**, 85–106.

Farquhar G. D., Ehleringer J. R. and Hubick K. T. (1989) Carbon isotope discrimination and photosynthesis. *Ann. Rev. Plant Physiol. Plant Mol. Biol.* **40**, 503–538.

Girard V., Schmidt A. R., Saint-Martin S., Struwe S., Perrichot V., Saint-Martin J. P., Breton G. and Néraudeau D. (2008) Exceptional preservation of marine diatoms in upper Albian amber. *Proc. Natl. Acad. Sci.* **105**, 17426–17429.

Glasspool I. J. and Scott A. C. (2010) Phanerozoic concentrations of atmospheric oxygen reconstructed from sedimentary charcoal. *Nat. Geosci.* **3**, 627–630.

Gomez B., Barale G., Saad D. and Perrichot V. (2003) Santonian Angiosperm-dominated leaf-assemblage from Piolenc (Vaucluse, Sud-Est de la France). *C.R. Palevol* **2**(3), 197–204.

Gradstein F. M., Ogg J. G., Schmitz M. and Ogg G. (2012) *The Geologic Time Scale 2012 2-Volume Set*, first ed. Elsevier.

Gröcke D. R. (1998) Carbon-isotope analyses of fossil plants as a chemostratigraphic and palaeoenvironmental tool. *Lethaia* **31**, 1–13.

Gröcke D. R. (2002) The carbon isotope composition of ancient CO_2 based on higher-plant organic matter. *Philos. Trans. Royal Soc. A* **360**, 633–658.

Gröcke D. R., Hesselbo S. P. and Jenkyns H. C. (1999) Carbonisotope composition of Lower Cretaceous fossil wood: Oceanatmosphere chemistry and relation to sea-level change. *Geology* **27**, 155–158.

Hall G., Woodborne S. and Scholes M. (2008) Stable carbon isotope ratios from archeological charcoals as palaeoenvironmental indicators. *Chem. Geol.* **247**, 384–400.

Hesselbo S. P., Jenkyns H. C., Duarte L. V. and Oliveira L. C. (2007) Carbon-isotope record of the Early Jurassic (Toarcian) Oceanic Anoxic Event from fossil wood and marine carbonate (Lusitanian Basin, Portugal). *Earth Planet. Sci. Lett.* **253**, 455–470.

Hultine K. R. and Marshall J. D. (2000) Altitude trends in conifer leaf morphology and stable carbon isotope composition. *Oecologia* **123**, 32–40.

Jahren A. H., Arens N. C. and Harbeson S. A. (2008) Prediction of atmospheric $\delta^{13}CO_2$ using fossil plant tissues. *Rev. Geophys.* **46**, RG1002. http://dx.doi.org/10.1029/2006RG000219.

Jones T. P. and Chaloner W. G. (1991) Fossil charcoal, its recognition and palaeoatmospheric significance. *Palaeogeogr. Palaeoclimatol. Palaeoecol.* **97**, 39–50.

Koch G. W., Sillett S. C., Jennings G. M. and Davis S. D. (2004) The limits to tree height. *Nature* **428**, 851–854.

Kohn M. J. (2010) Carbon isotope compositions of terrestrial C3 plants as indicators of (paleo)ecology and (paleo)climate. *Proc. Natl. Acad. Sci.* **107**, 19691–19695.

Kohn M. J. (2016) Carbon isotope discrimination in C3 land plants is independent of natural variations in pCO2. *Geochem. Perspect. Lett.* **2**, 35–43.

Körner C., Farquhar G. D. and Roksandic Z. (1988) A global survey of carbon isotope discrimination in plants from high altitude. *Oecologia* **74**, 623–632.

Körner C., Farquhar G. D. and Wong S. C. (1991) Carbon isotope discrimination by plants follows latitudinal and altitudinal trends. *Oecologia* **88**, 30–40.

Krzywinski M. and Altman N. (2014) Visualizing samples with box plots. *Nat. Methods* **11**, 119–120.

Lambert J. B., Santiago-Blay J. A. and Anderson K. B. (2008) Chemical signatures of fossilized resins and recent plant exudates. *Angew. Chem. Int. Ed.* **47**, 9608–9616.

Langenheim J. H. (1990) Plant resins. *Am. Sci.* **78**, 16–24.

Leavitt S. W. and Long A. (1986) Stable-carbon isotope variability in tree foliage and wood. *Ecology* **67**(4), 1002–1010.

Li X., Jenkyns H. C., Zhang C., Wang Y., Liu L. and Cao K. (2013) Carbon isotope signatures of pedogenic carbonates from SE China: rapid atmospheric pCO_2 changes during the middle-late Early Cretaceous time. *Geol. Mag.* **115**, 830–849.

Maksoud S., Granier B., Azar D., Gèze R., Paicheler J.-C. and Bedmar J. A. M. (2014) Revision of "Falaise de Blanche" (Lower Cretaceous) in Lebanon, with definition of a Jezzin regional Stage. *Carnets de Géologie* **14**, 401–427.

Maksoud S., Azar D., Granier B. and Gèze R. (2016) New data on the age of the Lower Cretaceous amber outcrops of Lebanon. *Palaeoworld*. http://dx.doi.org/10.1016/j.palwor.2016.03.003.

McElwain J. C., Willis K. J., Lupia R. and Muehlenbachs K. (2005) Cretaceous CO_2 decline and the radiation and diversification of Angiosperms. In *A history of atmospheric CO2 and its effects on plants, animals, and ecosystems* (eds. J. R. Ehleringer, T. E. Cerling and M. D. Dearing). Springer, New York, pp. 133–165.

Mckellar R. C., Wolfe A. P., Tappert R. and Muehlenbachs K. (2008) Correlation of Grassy Lake and Cedar Lake ambers using infrared spectroscopy, stable isotopes, and palaeontomology. *Can. J. Earth Sci.* **45**, 1061–1082.

McKellar R. C., Wolfe A. P., Muehlenbachs K., Tappert R., Engel M. S., Cheng T. and Sanchez-Azofeifa A. (2011) Insect outbreaks produce distinctive carbon isotope signatures in defencive resins and fossiliferous ambers. *Proc. R. Soc. B.* **278**, 3219–3224. http://dx.doi.org/10.1098/rspb.2011.0276.

Murray A. P., Padley D., McKirdy D. M., Booth W. E. and Summons R. E. (1994) Oceanic transport of fossil dammar resin: the chemistry of coastal resinites from South Australia. *Geochim. Cosmochim. Acta* **58**, 3049–3059.

Murray A. P., Edwards D., Hope J. M., Boreham C. J., Booth W. E., Alexander R. A. and Summons R. E. (1998) Carbon isotope biogeochemistry of plant resins and derived hydrocarbons. *Org. Geochem.* **29**, 1199–1214.

Néraudeau D., Vullo R., Gomez B., Girard V., Lak M., Videt B., Dépré E. and Perrichot V. (2009) Amber, plant and vertebrate fossils from the Lower Cenomanian paralic facies of Aix Island (Charente-Maritime, SW France). *Geodiversitas* **31**(1), 13–27.

Nissenbaum A. and Yakir D. (1995) Stable isotope composition of amber. In *Amber, resinite, and fossil resins. ACS Symposium series* (eds. K. B. Anderson and J. C. Crelling). American Chemical Society, Washington, pp. 32–42.

Nohra Y. A., Perrichot V., Jeanneau L., Le Pollès L. and Azar D. (2015) Chemical characterization and botanical origin of French ambers. *J. Nat. Prod.* **78**(6), 1284–1293.

Nordt L., Tubbs J. and Dworkin S. (2016) Stable carbon isotope record of terrestrial organic materials for the lest 450 Ma yr. *Earth Sci. Rev.* **159**, 103–117.

Peñalver E. and Delclòs X. (2010) Spanish amber. In *Biodiversity of Fossils in Amber from the Major World Deposits* (ed. D. Penney). Siri Scientific Press, Manchester, pp. 236–271.

Peyrot D., Jolly D. and Barron E. (2005) Apport de données palynologiques à la reconstruction paléoenvironnementale de l'Albo-Cénomanien des Charentes (Sud-Ouest de la France). *C. R. Palevol* **4**, 151–165.

Prokoph A., Shields G. A. and Veizer J. (2008) Compilation and time-series analysis of marine carbonate $\delta^{18}O$, $\delta^{13}C$, $^{87}Sr/^{86}Sr$ and $\delta^{34}S$ database through Earth history. *Earth Sci. Rev.* **87**, 113–133.

Ragazzi E. and Schmidt A. R. (2011) Amber. In *Encyclopedia of Geobiology* (eds. J. Reitner and V. Thiel). Springer, The Netherlands, pp. 24–36.

Retallack G. (2009) Greenhouse crises of the past 300 million years. *Geol. Soc. Am. Bull.* **121**, 1441–1455.

Rodríguez-López J. P., Meléndez N., Soria A. R. and de Boer P. L. (2009) Reinterpretación estratigráfica y sedimentológica de las formaciones Escucha y Utrillas de la Cordillera Ibérica. *Revista de la Sociedad Geológica de España* **22**, 163–219.

Saint Martin S., Saint Martin J. P., Girard V. and Néraudeau D. (2013) Organismes filamenteux de l'ambre du Santonien de Belcodène (Bouches-du-Rhône, France). *Annales de Paléontologie* **99**(4), 339–359.

Salazar-Jaramillo S., Fowell S. J., McCarthy P. J., Benowitz J. A., Sliwinski M. G. and Tomisich C. S. (2016) Terrestrial isotopic evidence for a Middle-Maastrichtian warming event from the lower Cantwell Formation, Alaska. *Palaeogeogr. Palaeoclimatol. Palaeoecol.* **441**, 360–376.

Scalarone D., van der Horst J., Boon J. J. and Chiantore O. (2003) Direct-temperature mass spectrometric detection of volatile terpenoids and natural terpenoid polymers in fresh and artificially aged resins. *J. Mass Spectrom.* **38**, 607–617.

Schubert B. A. and Jahren A. H. (2012) The effect of atmospheric CO2 concentration on carbon isotope fractionation in C3 land plants. *Geochim. Cosmochim. Acta* **96**, 29–43.

Schubert B. A. and Jahren A. H. (2013) Reconciliation of marine and terrestrial carbon isotope excursions based on changing atmospheric CO_2 levels. *Nat. Commun.* **4**, 1653. http://dx.doi.org/10.1038/ncomms2659.

Schubert B. A. and Jahren A. H. (2015) Global increase in carbon isotope fractionation following the Last Glacial Maximum caused by increase in atmospheric pCO_2. *Geology* **43**, 435–438.

Scotese C.R. (2002) http://www.scotese.com, (PALEOMAP website).

Spiker E. C. and Hatcher P. G. (1987) The effects of early diagenesis on the chemical and stable carbon isotopic composition of wood. *Geochim. Cosmochim. Acta* **51**, 1385–1391.

Stern B., Lampert Moore C. D., Heron C. and Pollard A. M. (2008) Bulk stable light isotopic ratios in recent and archaeological resins: towards detecting the transport of resins in antiquity? *Archaeometry* **50**, 351–370.

Strauss H. and Peters-Kottig W. (2003) The Paleozoic to Mesozoic carbon cycle revisited: the carbon isotopic composition of terrestrial organic matter. *Geochem. Geophys. Geosyst.* **4**(10), 1083. http://dx.doi.org/10.1029/2003GC000555.

Tappert R., McKellar R., Wolfe A. P., Tappert M. C., Ortega-Blanco J. and Muehlenbachs K. (2013) Stable carbon isotopes of C3 plant resins and ambers record changes in atmospheric oxygen since the Triassic. *Geochim. Cosmochim. Acta* **121**, 240–262.

Tipple B. J. and Pagani M. (2007) The early origins of terrestrial C4 photosynthesis. *Annu. Rev. Earth Planet. Sci.* **35**, 435–461.

Tipple B. J., Meyers S. R. and Pagani M. (2010) Carbon isotope ratio of Cenozoic CO_2: a comparative evaluation of available geochemical proxies. *Paleoceanography* **25**, PA3202. http://dx.doi.org/10.1029/2009PA001851.

van Bergen P. F. and Poole I. (2002) Stable carbon isotopes of wood: a clue to palaeoclimate? *Palaeogeogr. Palaeoclimatol. Palaeoecol.* **182**, 31–45.

Villanueva-Amadoz U., Pons D., Diez J. B., Ferrer J. and Sender L. M. (2010) Angioperm pollen grains of San just (Escucha Formation) from the Albian of the Iberian Range (northeastern Spain). *Rev. Palaeobot. Palynol.* **162**, 362–381.

Wallmann K. (2001) Controls on the Cretaceous and Cenozoic evolution of seawater composition, atmospheric CO_2 and climate. *Geochim. Cosmochim. Acta* **18**, 3005–3025.

Wang Y., Huang C., Sun B., Quan C., Wu J. and Lin Z. (2014) Paleo-CO$_2$ variation trends and the Cretaceous greenhouse climate. *Earth Sci. Rev.* **129**, 136–147.

Warren C. R., McGrath J. F. and Adams M. A. (2001) Water availability and carbon isotope discrimination in conifers. *Oecologia* **127**, 476–486.

Yans J., Gerards T., Gerrienne P., Spagna P., Dejax J., Schnyder J., Storme J.-Y. and Keppens E. (2010) Carbon-isotope analysis of fossil wood and dispersed organic matter from the terrestrial Wealden facies of Hautrage (Mons Basin, Belgium). *Palaeo-geogr. Palaeoclimatol. Palaeoecol.* **291**, 85–105.

Zhang J. W. and Cregg B. M. (1996) Variation in stable isotope discrimination among and within exotic conifer species grown in eastern Nebraska, USA. *For. Ecol. Manage.* **83**, 181–187.

Associate editor: Alex L. Sessions